

**IAEA**

International Atomic Energy Agency

# Nuclear–Wind Hybrid Energy System Part-Task Simulator

*Manual and Practical Exercises*

VIENNA, 2023

TRAINING COURSE SERIES

**79**

NUCLEAR–WIND HYBRID ENERGY  
SYSTEM PART-TASK SIMULATOR

The following States are Members of the International Atomic Energy Agency:

AFGHANISTAN	GAMBIA	OMAN
ALBANIA	GEORGIA	PAKISTAN
ALGERIA	GERMANY	PALAU
ANGOLA	GHANA	PANAMA
ANTIGUA AND BARBUDA	GREECE	PAPUA NEW GUINEA
ARGENTINA	GRENADA	PARAGUAY
ARMENIA	GUATEMALA	PERU
AUSTRALIA	GUYANA	PHILIPPINES
AUSTRIA	HAITI	POLAND
AZERBAIJAN	HOLY SEE	PORTUGAL
BAHAMAS	HONDURAS	QATAR
BAHRAIN	HUNGARY	REPUBLIC OF MOLDOVA
BANGLADESH	ICELAND	ROMANIA
BARBADOS	INDIA	RUSSIAN FEDERATION
BELARUS	INDONESIA	RWANDA
BELGIUM	IRAN, ISLAMIC REPUBLIC OF	SAINT KITTS AND NEVIS
BELIZE	IRAQ	SAINT LUCIA
BENIN	IRELAND	SAINT VINCENT AND THE GRENADINES
BOLIVIA, PLURINATIONAL STATE OF	ISRAEL	SAMOA
BOSNIA AND HERZEGOVINA	ITALY	SAN MARINO
BOTSWANA	JAMAICA	SAUDI ARABIA
BRAZIL	JAPAN	SENEGAL
BRUNEI DARUSSALAM	JORDAN	SERBIA
BULGARIA	KAZAKHSTAN	SEYCHELLES
BURKINA FASO	KENYA	SIERRA LEONE
BURUNDI	KOREA, REPUBLIC OF	SINGAPORE
CABO VERDE	KUWAIT	SLOVAKIA
CAMBODIA	KYRGYZSTAN	SLOVENIA
CAMEROON	LAO PEOPLE'S DEMOCRATIC REPUBLIC	SOUTH AFRICA
CANADA	LATVIA	SPAIN
CENTRAL AFRICAN REPUBLIC	LEBANON	SRI LANKA
CHAD	LESOTHO	SUDAN
CHILE	LIBERIA	SWEDEN
CHINA	LIBYA	SWITZERLAND
COLOMBIA	LIECHTENSTEIN	SYRIAN ARAB REPUBLIC
COMOROS	LITHUANIA	TAJIKISTAN
CONGO	LUXEMBOURG	THAILAND
COSTA RICA	MADAGASCAR	TOGO
CÔTE D'IVOIRE	MALAWI	TONGA
CROATIA	MALAYSIA	TRINIDAD AND TOBAGO
CUBA	MALI	TUNISIA
CYPRUS	MALTA	TÜRKİYE
CZECH REPUBLIC	MARSHALL ISLANDS	TURKMENISTAN
DEMOCRATIC REPUBLIC OF THE CONGO	MAURITANIA	UGANDA
DENMARK	MAURITIUS	UKRAINE
DJIBOUTI	MEXICO	UNITED ARAB EMIRATES
DOMINICA	MONACO	UNITED KINGDOM OF GREAT BRITAIN AND NORTHERN IRELAND
DOMINICAN REPUBLIC	MONGOLIA	UNITED REPUBLIC OF TANZANIA
ECUADOR	MONTENEGRO	UNITED STATES OF AMERICA
EGYPT	MOROCCO	URUGUAY
EL SALVADOR	MOZAMBIQUE	UZBEKISTAN
ERITREA	MYANMAR	VANUATU
ESTONIA	NAMIBIA	VENEZUELA, BOLIVARIAN REPUBLIC OF
ESWATINI	NEPAL	VIET NAM
ETHIOPIA	NETHERLANDS	YEMEN
FIJI	NEW ZEALAND	ZAMBIA
FINLAND	NICARAGUA	ZIMBABWE
FRANCE	NIGER	
GABON	NIGERIA	
	NORTH MACEDONIA	
	NORWAY	

The Agency's Statute was approved on 23 October 1956 by the Conference on the Statute of the IAEA held at United Nations Headquarters, New York; it entered into force on 29 July 1957. The Headquarters of the Agency are situated in Vienna. Its principal objective is "to accelerate and enlarge the contribution of atomic energy to peace, health and prosperity throughout the world".

TRAINING COURSE SERIES No. 79

NUCLEAR–WIND HYBRID ENERGY  
SYSTEM PART-TASK SIMULATOR  
MANUAL AND PRACTICAL EXERCISES

INTERNATIONAL ATOMIC ENERGY AGENCY  
VIENNA, 2023

## COPYRIGHT NOTICE

All IAEA scientific and technical publications are protected by the terms of the Universal Copyright Convention as adopted in 1952 (Berne) and as revised in 1972 (Paris). The copyright has since been extended by the World Intellectual Property Organization (Geneva) to include electronic and virtual intellectual property. Permission to use whole or parts of texts contained in IAEA publications in printed or electronic form must be obtained and is usually subject to royalty agreements. Proposals for non-commercial reproductions and translations are welcomed and considered on a case-by-case basis. Enquiries should be addressed to the IAEA Publishing Section at:

Marketing and Sales Unit, Publishing Section  
International Atomic Energy Agency  
Vienna International Centre  
PO Box 100  
1400 Vienna, Austria  
fax: +43 1 26007 22529  
tel.: +43 1 2600 22417  
email: [sales.publications@iaea.org](mailto:sales.publications@iaea.org)  
[www.iaea.org/publications](http://www.iaea.org/publications)

For further information on this publication, please contact:

Nuclear Power Technology Development Section  
International Atomic Energy Agency  
Vienna International Centre  
PO Box 100  
1400 Vienna, Austria  
Email: [Official.Mail@iaea.org](mailto:Official.Mail@iaea.org)

NUCLEAR–WIND HYBRID ENERGY SYSTEM PART-TASK SIMULATOR: MANUAL AND PRACTICAL EXERCISES  
IAEA, VIENNA, 2023  
IAEA-TCS-79  
ISSN 1018–5518

© IAEA, 2023

Printed by the IAEA in Austria  
November 2023

## FOREWORD

The IAEA offers its Member States a wide spectrum of education and training activities. These include face-to-face training courses and workshops, on-line learning, fellowship programmes and schools, as well as publications in the IAEA's Training Course Series, including handbooks, textbooks and manuals on various nuclear related topics.

Experience shows that education and training supported by hands-on learning by doing using nuclear power plant simulators is an effective way for a broad range of target groups to meet education and training standards. The IAEA regularly publishes reference material and holds training courses to assist professionals in Member States in understanding nuclear power plant simulators and associated technologies. The education and training courses support an integrated approach that combines lectures with learning by doing on the specifics of plant operation, including reactor physics, thermal hydraulics and safety aspects, using basic principle simulators.

Classification, Selection and Use of Nuclear Power Plant Simulators for Education and Training (IAEA-TECDOC-1887) provides information for educational institutions, training centres and suppliers on the proper classification, selection and use of various types of nuclear power plant simulators. The IAEA also provides opportunities for hands-on learning using nuclear reactor simulation computer programs, either full plant basic principle simulators or part-task simulators addressing specific parts of plant operations (i.e. systems or components) or specific phenomena. The simplified reactor designs of basic principle simulators allow professionals to grasp fundamental concepts without becoming overwhelmed by the details of a more complex, full scope simulator. The objective of these basic principle full plant or part-task simulators is to provide insight into and a practical understanding of the operational characteristics of reactors as well as plant responses to perturbations and accident scenarios. Access to both types of basic principle simulator is available to Member States upon request, and thus represents a valuable resource for teaching and training on a wide range of topics relevant to nuclear power plant design, safety, technology, simulation and operations.

This publication provides a comprehensive explanation of the nuclear-wind hybrid energy system part-task simulator as well as practical exercises to help readers become familiar with its use. By engaging in these exercises with the part-task simulator, readers will gain hands-on experience and a deeper understanding of its workings.

The IAEA acknowledges the contributions of the Department of Nuclear Engineering at Pakistan Institute of Engineering and Applied Sciences in the development of the part-task simulator described in this publication.

The IAEA officer responsible for this publication was T. Jevremovic of the Division of Nuclear Power.

## *EDITORIAL NOTE*

*This publication has been prepared from the original material as submitted by the contributors and has not been edited by the editorial staff of the IAEA. The views expressed remain the responsibility of the contributors and do not necessarily reflect those of the IAEA or the governments of its Member States.*

*Guidance and recommendations provided here in relation to identified good practices represent expert opinion but are not made on the basis of a consensus of all Member States.*

*Neither the IAEA nor its Member States assume any responsibility for consequences which may arise from the use of this publication. This publication does not address questions of responsibility, legal or otherwise, for acts or omissions on the part of any person.*

*The use of particular designations of countries or territories does not imply any judgement by the publisher, the IAEA, as to the legal status of such countries or territories, of their authorities and institutions or of the delimitation of their boundaries.*

*The mention of names of specific companies or products (whether or not indicated as registered) does not imply any intention to infringe proprietary rights, nor should it be construed as an endorsement or recommendation on the part of the IAEA.*

*The authors are responsible for having obtained the necessary permission for the IAEA to reproduce, translate or use material from sources already protected by copyrights.*

*The IAEA has no responsibility for the persistence or accuracy of URLs for external or third party Internet web sites referred to in this publication and does not guarantee that any content on such web sites is, or will remain, accurate or appropriate.*

## CONTENTS

1.	INTRODUCTION .....	1
1.1.	BACKGROUND .....	1
1.2.	OBJECTIVE .....	2
1.3.	SCOPE.....	2
1.4.	STRUCTURE .....	2
2.	HYBRID ENERGY SYSTEMS.....	2
2.1.	HISTORICAL BACKGROUND .....	2
2.2.	PROMINENT CHARACTERISTICS OF NUCLEAR-WIND HYBRID ENERGY SYSTEM WITHIN THE PART-TASK SIMULATOR .....	4
2.2.1.	Wind farm .....	5
2.2.2.	Small modular reactor.....	5
2.2.3.	Regulating node .....	6
2.2.4.	Hydrogen production plant .....	7
2.2.5.	Biomass processing plant.....	7
2.3.	LIMITATIONS AND ASSUMPTIONS .....	9
3.	GENERAL INSTRUCTIONS.....	10
3.1.	INSTALLATION .....	10
3.2.	START UP .....	10
3.3.	MODES .....	11
3.3.1.	Simulator mode.....	11
3.3.2.	Test SMR mode .....	13
4.	EXAMPLES .....	15
4.1.	INSTANANEOUS WIND SPEED AND LOAD (SIMULATOR MODE) .....	16
4.1.1.	Simulation steps.....	16
4.1.2.	Analysis of the output parameters .....	17
4.2.	YEARLY WIND SPEED AND LOAD DATA (TEST SMR MODE)...	18
4.2.1.	Simulation steps.....	20
4.2.2.	Analysis of the output parameters .....	20
4.3.	VARIABLE BIOMASS AND ENERGY REQUIREMENTS FOR PROCESSING.....	22
4.3.1.	Simulation steps.....	22
4.3.2.	Analysis of the output parameters .....	23
4.4.	EFFECT OF INITIAL MOISTURE CONTENT ON THERMAL ENERGY UTILIZATION FOR BIOMASS PROCESSING (SMR MODE) .....	24
4.4.1.	Simulation steps.....	24
4.4.2.	Analysis of the output parameters .....	25
4.5.	EFFECT OF HYDROGEN REQUIREMENT ON SYNTHETIC FUEL PRODUCTION (SMR MODE).....	26
4.5.1.	Simulation steps.....	26
4.5.2.	Analysis of the output parameters .....	26
	REFERENCES.....	29



ANNEX I .....31

ANNEX II .....39

CONTRIBUTORS TO DRAFTING AND REVIEW .....43

# 1. INTRODUCTION

## 1.1. BACKGROUND

In support of human resource development in Member States, the IAEA has established education and training programmes on active learning about nuclear technologies using basic principle nuclear power plant and part-task simulators. As part of this programme, the IAEA arranges for the development and distribution of its suites of basic principle simulators including the manuals and related documentation, supports education and training courses and workshops on physics and technology of advanced reactors, methodology on technology assessment and technology relevant databases.

Hands-on learning using nuclear power plant simulators has become an essential tool for education and training programmes worldwide. Experience shows that simulators are effective in allowing a broad range of target groups to meet education and training standards. The International Atomic Energy Agency (IAEA) has been at the forefront of promoting and supporting the use of simulators for education and training purposes. The IAEA TECDOC-1887 on Classification, Selection and Use of Nuclear Power Plant Simulators for Education and Training provides guidance for educational institutions, training centres, and suppliers on the proper classification, selection, and use of various types of simulators [1]. The IAEA assists Member States by providing education and training courses on the physics and technology of nuclear power plant operation through hands-on learning with nuclear reactor simulation computer programs. The programs may refer to full plant basic principle simulators or to part-task simulators addressing specific parts of plant operations (systems or components) or specific phenomena. Both types of basic principle simulators are available to Member States upon request, representing an accessible resource for teaching and training on a wide range of topics relevant to nuclear power plant design, safety, technology, simulation, and operations. The basic principle simulators available through the IAEA often feature simplified reactor designs, allowing professionals to grasp fundamental concepts without becoming overwhelmed by the details of a more complex, full-scope simulator. The objective of these simulators is to provide insight into and a practical understanding of reactor operational characteristics and plant responses to transient and accident scenarios. This type of learning is critical for nuclear power plant personnel, who must be trained to respond quickly and appropriately in transient and accidental conditions. The IAEA regularly publishes reference material and holds education and training courses to assist professionals in Member States in understanding simulators and associated technologies. Education and training courses support an integrated approach that combines lectures with learning by doing on the specifics of plant operation, including reactor physics, thermal hydraulics, and safety aspects, using basic principle simulators.

This publication provides description relevant to understanding basic principles of HES configuration and working, in which nuclear power plant and renewable energy source are coupled to work in synergy to produce desirable outputs. Detailed description of nuclear-wind HES part-task simulator is provided together with the exercises applicable to education and training courses and workshops, or self-learning.

## 1.2. OBJECTIVE

The objectives of this publication are to:

- Serve as a reference for lectures on basic principles of HES configuration and operation.
- Support Member States intending to use IAEA part-task simulators in national education and training programmes with a resource for necessary background information on theory of HES operation;
- Serve as a reference for students and trainees, who may be unfamiliar with reactor operation in synergy with renewable energy source (e.g., engineering safety, physical sciences, non-nuclear engineering fields, and including non-technical fields) to understand the integration of nuclear with renewables at a basic level;
- Provide exercises for use in education and training courses, use by Member State institutions, or direct use by students or trainees.

## 1.3. SCOPE

The scope of this publication is to explain the underlying phenomena, modelling methodology, and application of nuclear-wind HES. Explanations and examples are limited to the part-task simulator options. Other similar publications address different types of nuclear-renewable HES. Following and overview of HES configuration and operation, this publication provides explanations about the part-task simulator and examples to study.

## 1.4. STRUCTURE

This publication contains descriptions about:

- **Hybrid energy systems (Section 2)** which provides general purpose overview and designs, such as the basic configuration and function of systems and components, relevant to later explanations;
- **General Instructions (Section 3)** regarding nuclear-wind part-task simulator including its configuration, modelled systems, and installation;
- **Examples (Section 4)** containing practical exercises of various HES analysis and functions, with explanations about the parameter trends and values.

# 2. HYBRID ENERGY SYSTEMS

## 2.1. HISTORICAL BACKGROUND

Nuclear energy and renewables are the two principal options for low carbon energy generation. The concept of integrating two or more energy sources to form a cooperatively controlled multisource system providing responsive generation to the power grid is referred to as HES [2]. Nuclear-renewable HES consider opportunities to couple these energy generation sources to leverage the benefits of each technology to provide reliable, sustainable electricity to the grid and to provide low carbon energy to other energy use sectors as discussed in the IAEA Nuclear

Energy Series on Nuclear-Renewable Hybrid Energy Systems [3]. Nuclear-renewable HESs can produce heat, electricity, and other products that society requires while supporting higher penetrations of variable renewable generation. Such systems therefore can provide energy to support various applications, such as seawater or brackish water desalination, hydrogen production, district heating or cooling, the extraction of tertiary oil resources, and process heat applications such as cogeneration, coal-to-liquids conversion, and assistance in the synthesis of chemical feedstock [3]. Various HES are studied in the past and their configurations analysed from technology and economic aspects: Neto, et al. [4] discussed several examples of how HESs can be used worldwide, Nixon et al. provided in-depth analysis regarding technical challenges, opportunities and feasibility studies of various HESs [5], and some other examples of HES are described by Rehman and Al-Hadhrami [6], Zoubeidi et al. [7], and Kaledellis and Kavadia [8].

There are large hybridized electrical facilities that are integrating fossil fired power plants with renewables. However, a major cause of global climate change is due to the emissions of greenhouse gases. The main contributor to global warming is the fossil fired power plants which account for about one-quarter of total emissions of CO<sub>2</sub> [9]. The advanced coal-fired and natural-gas fired power plants will eventually require advanced carbon capturing techniques to meet the global greenhouse gases emission goals. To protect the environment, efforts are now shifted towards nuclear-renewable HES that can provide innovative technical and improved economic solutions to greenhouse gases emissions as compared to only-electricity power plants. Additionally, one of the major problems of using renewable energy sources is their intermittent nature. This causes load variations at the grid. Nuclear-renewable HES are able to provide the dispatchable generation to meet the needs for electric grid by rapidly increasing or decreasing electricity outputs. Nuclear-renewable HES can also provide flexibility by integration with industrial applications [10].

Nuclear-renewable HES consists of a nuclear power source, turbine, at least one renewable energy source and an industrial process for utilization of power. These systems may or may not be geographically correlated. Nuclear-renewable HES can be grouped into three general categories: tightly coupled HES in which nuclear-renewable generation sources and the industrial processes are directly coupled behind the grid with single connection point to the grid, thermally coupled HES in which heat generation sources are tightly coupled behind the grid, whereas the grid can have multiple connections from different renewable energy sources, and loosely coupled HES in which there is no direct thermal coupling [10].

Cherry et al. [11] presented one of the concepts of nuclear-renewable HES, in which the core ability of the HES was to efficiently shift heat energy produced by nuclear reactor between electricity production and synthetic fuel production depending on the load requirements. A similar evaluation is also performed by Carlsson et al. [12] in which a combination of tightly coupled and loosely coupled nuclear-renewable HES comprising of wind, nuclear, and biomass plants is considered for effective load following and production of synthetic fuels. This nuclear-renewable HES is used as a basic concept for nuclear-wind HES part-task simulator described in this publication.

## 2.2. PROMINENT CHARACTERISTICS OF NUCLEAR-WIND HYBRID ENERGY SYSTEM WITHIN THE PART-TASK SIMULATOR

The nuclear-wind HES consists of a wind farm, small modular reactor (SMR), biomass processing plant, and a hydrogen production plant. The renewable energy source (windfarm) is integrated with the SMR behind the grid to reduce its intermittency. The provision of a biomass processing plant allows the SMR to operate at its full thermal power. This HES is designed to fulfill the load requirement at the grid by sending the excess electricity and excess thermal energy to the hydrogen production plant and the biomass processing plant, respectively for the effective load following. The low wind power production is compensated by SMR supplying the steam to turbine to increase electrical power production. When wind generation increases, SMR reduces electricity production and supplies heat to the biomass processing plant. A complete layout of this HES system as used in the part-task simulator is shown in Fig. 1. It is to be mentioned that it is a conceptual integrated HES with a multiple stage steam extraction system.

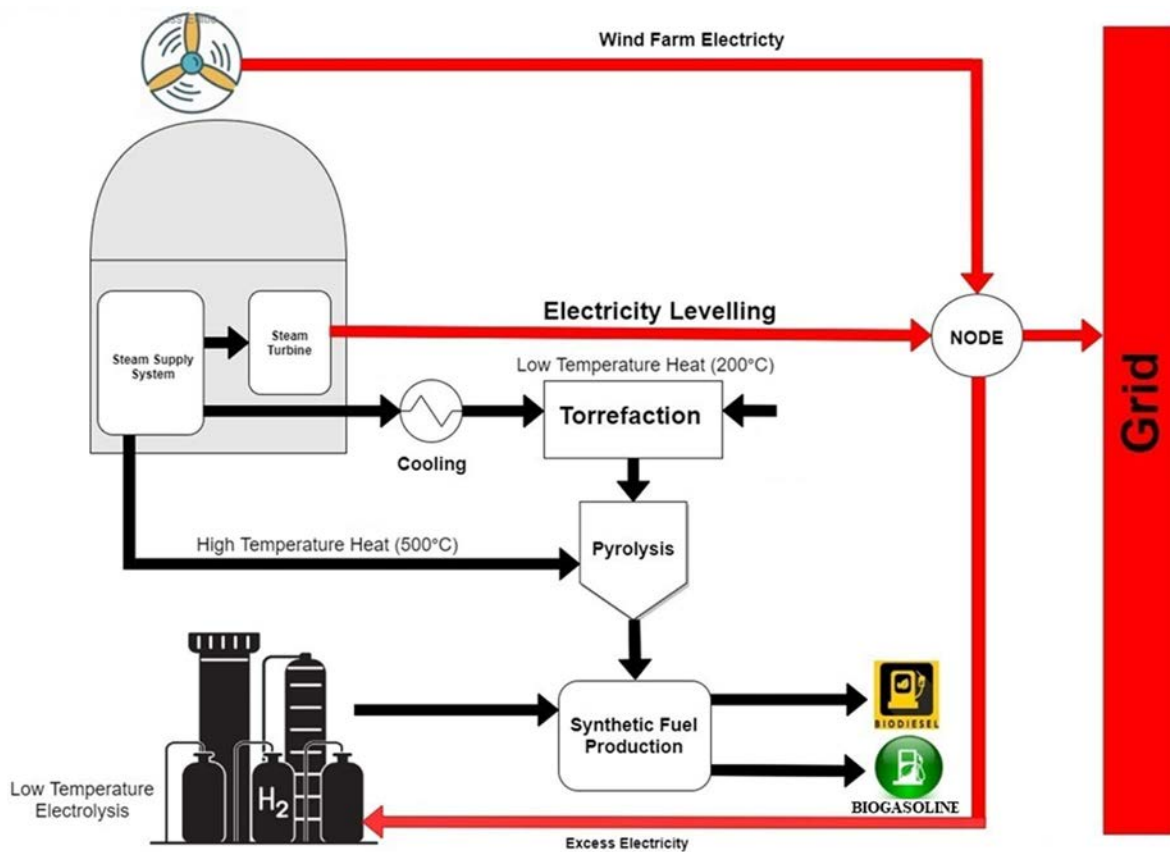


FIG. 1. Configuration and layout of the nuclear-wind HES.

The constraints in the analysis performed by this part-task simulator are:

- Turbine output of the nuclear reactor cannot be decreased below 30% of its rated capacity;
- SMR always operates at full thermal power output;

- Turbine output is varied by diverting the excess heat towards the biomass processing plant in the hours of low electricity demand;
- As turbine output cannot be decreased below 30% of its rated capacity, the generated excess electricity is used to produce hydrogen based on the low temperature electrolysis.

### 2.2.1. Wind farm

Onshore or offshore wind farm (or wind park, or wind power station, or wind power plant) consists of wind generators ranging from 600 kW to 5 MW that are combined in one location to produce electricity. General description of a wind farms is provided in Annex I.

Two inputs are required to compute the electrical output obtained from the wind farm:

- Rated capacity of the wind farm;
- Wind speed.

Corresponding to the user-defined rated capacity and wind speed, the electrical output from the wind farm can be computed using the data from FIG. 2 [13].

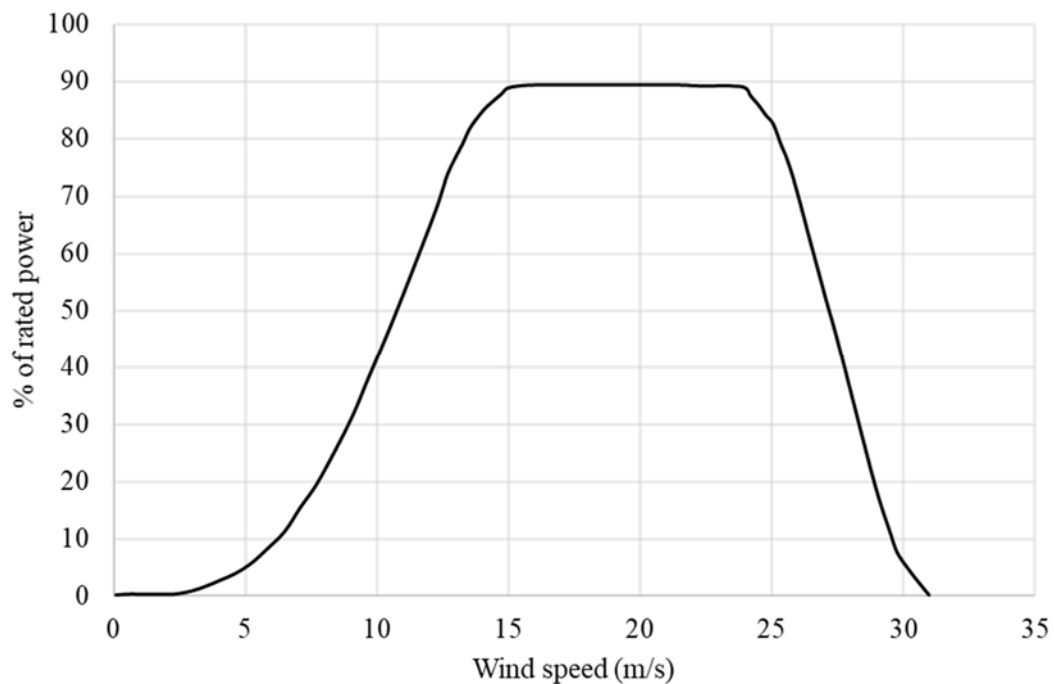


FIG. 2. Windfarm power production trends.

### 2.2.2. Small modular reactor

Since high temperature pyrolysis is performed in the biomass processing plant, the steam output temperature from the turbines is in the range that high temperature pyrolysis can be performed. The main purpose of the SMR is to compensate for the intermittent output from the windfarm

such that the load requirements at the grid are met. This is achieved by varying the electrical output from 30% to 100% of its rated capacity while diverting the excess heat energy towards biomass processing plant. The electrical and thermal outputs from SMR are:

- If the load requirement at the grid can be catered with wind farm's electrical output only, then:

$$\text{Net electrical output from SMR (MWe)} = 30\% \text{ of its rated power}$$

$$\text{Thermal output from SMR (MWth)} = [70\% \text{ of its rated power}] / 0.45, \text{ where } 45\% \text{ is the assumed overall SMR thermal efficiency.}$$

- If the load requirement at the grid cannot be catered with wind farm's electrical output only, then:

$$\text{Difference (MWe)} = [\text{Load requirement}] - [\text{Electrical output from the wind farm}]$$

- If the difference is greater than or equal to the rated capacity of SMR, then:

$$\text{SMR electrical output (MWe)} = 100\% \text{ of its rated capacity}$$

$$\text{SMR thermal output (MWth)} = 0$$

- If the difference is less than the rated capacity of the nuclear reactor or greater than 30% of the rated capacity of the reactor, then:

$$\text{SMR electrical output (MWe)} = \text{Difference}$$

$$\text{SMR thermal output (MWth)} = [\text{Rated capacity} - \text{Difference}] / 0.45$$

### **2.2.3. Regulating node**

The purpose of regulating node is to supply the electrical output from the wind farm and the SMR towards the grid as per demand while diverting the excess electrical output towards hydrogen production plant. Thus, total electrical supply towards the grid and hydrogen production plant is:

- If the load required at the grid is greater than or equal to the electrical output of the HES, then:

$$\text{Grid output (MWe)} = \text{Electrical output from the HES}$$

$$\text{Hydrogen plant input (MWe)} = 0$$

- If load required at the grid is less than the electrical output of the HES, then:

Grid input (MWe) = Required load at the grid

Hydrogen plant input (MWe) = [Output from HES] – [Required load at the grid]

#### 2.2.4. Hydrogen production plant

Hydrogen production plant uses the excess electricity produced by the HES. The introduction of the HES ensures effective load following during low load hours. Hydrogen production plant produces hydrogen via low temperature electrolysis in which water molecule is split into oxygen and hydrogen gas using electricity. Low temperature electrolysis usually involves alkaline electrolytic cell or proton exchange membrane cells. Details are provided in Annex II.

#### 2.2.5. Biomass processing plant

The introduction of biomass processing plant allows nuclear reactor (such as SMR) to operate at its full thermal capacity making its operation technically and economically feasible. In the biomass processing plant, the dried biomass first undergoes torrefaction followed by pyrolysis thereby producing bio-oil, biochar, and biogas. The bio-oil thus obtained is combined with the hydrogen produced using the excess electricity to produce biodiesel and bio gasoline. The schematics is shown in FIG. 3. The first step in biomass processing is drying and torrefaction. During drying process, the moisture content of the biomass is reduced. The dried biomass then undergoes torrefaction which is defined as: “thermochemical process in an inert or limited oxygen environment where biomass is slowly heated to within a temperature range of 200°C–300°C and retained there for a stipulated time such that it results in near complete degradation of its hemicellulose content while maximizing mass and energy yield of solid product” [14].

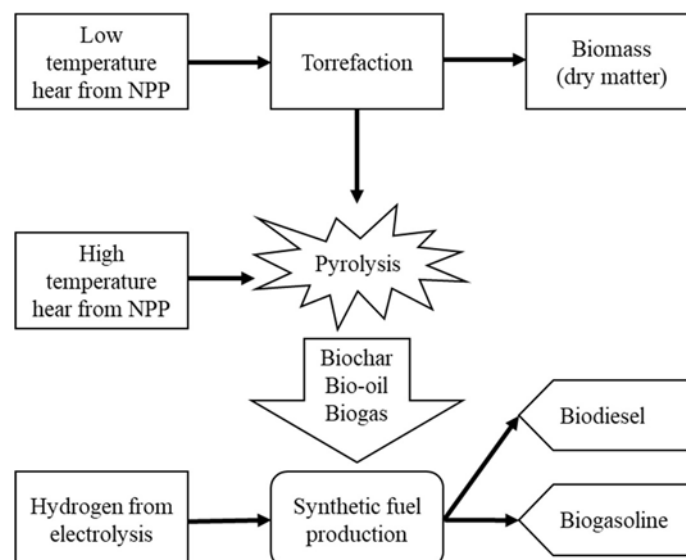


FIG. 3. Schematics of a biomass processing plant.

Typical heating rate for torrefaction is less than 50 °C/min which is considerably low compared to pyrolysis to maximize the yield of solid product. In torrefaction, products of high energy



density are obtained, which are suitable for biofuel production while some volatile organic compounds are released which are reused in the HES thus reducing the heat requirement as follows:

$$\text{Energy required to dry and torrefy } \left( \frac{\text{GWh}}{\text{year}} \right) = 0.0002778 \times \frac{E_{rd}(\text{BM} \times \text{DE})}{1-\text{IM}} \quad (1)$$

where:

BM: mass of dried biomass (dry matter tonne/ year)

IMC: initial moisture content of as-obtained biomass

DE: specific energy required for drying and torrefaction of the considered biomass (GJ/tonne of moist feed)

$E_{rd}$ : reduced energy requirement, which is assumed to be 0.27 (or 27%) [12], since it is assumed that combustible gases are reused after torrefaction.

The second step in biomass processing is pyrolysis, which involves heating the torrefied product at an elevated temperature in the absence of oxygen and retaining that temperature for a particular time to produce bio-oil, char, and non-condensable gases. The proportion of each product depends on the heating rate and temperature of pyrolysis. For example, the yield of char decreases at high pyrolysis temperatures whereas, slower heating results in greater amount of char. Pyrolysis is classified as slow or fast based on the heating rate. It is considered as fast if the time required to reach the pyrolysis temperature is much larger than the pyrolysis reaction time and vice-versa. In the simulator, fast pyrolysis is considered as it maximizes the production of bio-oil. Increasing the yield of bio-oil involves rapid heating (as high as 1,000°C–10,000°C) of feedstock (torrefied pellets) so that it attains the pyrolysis temperature before it undergoes decomposition. The pyrolysis is carried out at a moderate temperature (400°C–600°C) to increase the production of bio-oil. In this nuclear-wind HES, bio-oil is converted into synthetic fuel. Biochar and off-gas formed during pyrolysis are treated as by products. The energy required to perform pyrolysis for the given biomass can be calculated using the following:

$$\text{Energy required for pyrolysis } \left( \frac{\text{GWh}}{\text{year}} \right) = 0.0002778 \times \frac{(\text{BM} \times \text{PE})}{1-\text{MC}} \quad (2)$$

where PE is specific energy required for pyrolysis of the considered biomass (GJ/tonne of moist feed), and MC is moisture content of dried biomass. The products obtained during pyrolysis, biochar, bio-oil, and off-gas, can be calculated as follows:

$$\text{Char produced } \left( \frac{\text{tonnes}}{\text{year}} \right) = \frac{\text{PY} \times \text{BM}}{1-\text{MC}} \quad (3)$$

where PY is a specific yield of pyrolysis char (kg/kg of dried biomass), and

$$\text{Bio-oil produced } \left( \frac{\text{tonnes}}{\text{year}} \right) = \frac{\text{OY} \times \text{BM}}{1-\text{MC}} \quad (4)$$

where OY represents specific yield of bio-oil (kg/kg of dried biomass);

$$\text{Off-gas produced } \left( \frac{\text{tonnes}}{\text{year}} \right) = \frac{\text{GY} \times \text{BM}}{1 - \text{MC}} \quad (5)$$

and GY is a specific yield of off-gas (kg/kg of dried biomass). The last step of biomass processing is synthetic fuel production. In this step, hydrogen is used to convert the produced bio-oil into biodiesel and biogasoline. During this process, oxygen in the bio-oil combines with hydrogen to produce water, thus, converting the remaining biomass into biofuel. The electricity required to produce the required hydrogen is given with:

$$\text{Electricity required for low temperature electrolysis } \left( \frac{\text{GWh}}{\text{year}} \right) = E_{CH} \times \text{HR} \times \text{Bio-oil produced} \quad (6)$$

where is  $E_{CH}$ . electricity consumed (GWh) in producing one tonne of hydrogen which is 0.02177 [12], and HR defines a specific hydrogen consumption (tonnes of hydrogen/tonne of bio-oil). The products obtained during synthetic fuel production, biodiesel and biogasoline, can be calculated as follows:

$$\text{Biogasoline produced } \left( \frac{\text{m}^3}{\text{year}} \right) = \text{BGY} \times \text{Bio-oil produced} \quad (7)$$

where BGY is a specific yield of biogasoline ( $\text{m}^3/\text{tonne}$  of bio-oil). And,

$$\text{Biodiesel produced } \left( \frac{\text{m}^3}{\text{year}} \right) = \text{BDY} \times \text{Bio-oil produced} \quad (8)$$

where BDY is a specific yield of biodiesel ( $\text{m}^3/\text{tonne}$  of bio-oil). For biomass processing, default values for bagasse, produced in the province of Pakistan's, the Sindh province, are considered for the constants used in Eqs. (1)–(8):

$$\text{BM} = 1,136,166 \text{ [15]}$$

$$\text{IMC} = 0.5 \text{ [16]}$$

$$\text{MC} = 0.07 \text{ [12]}$$

$$\text{DE} = 0.83 \text{ GJ/tonne of moist feed [12]}$$

$$\text{PE} = 3.543 \text{ GJ/tonne of dried feed [17]}$$

$$\text{PY} = 0.2 \text{ kg/kg of dried biomass [18]}$$

$$\text{OY} = 0.6 \text{ kg/kg of dried biomass [18]}$$

$$\text{GY} = 0.17 \text{ kg/kg of dried biomass [18]}$$

$$\text{HR} = 0.05024 \text{ ton/ton of bio-oil [12]}$$

$$\text{BGY} = 0.2644 \text{ m}^3/\text{ton of bio-oil [12]}$$

$$\text{BDY} = 0.3365 \text{ m}^3/\text{ton of bio-oil [12]}$$

### 2.3. LIMITATIONS AND ASSUMPTIONS

The nuclear-wind HES part-task simulator observes the following limitations and assumptions:

- Overall thermal efficiency of the nuclear reactor is 45%;

- It is assumed that the combustible gases after torrefaction are reused reducing the energy requirement for drying and torrefaction to 27%;
- Hydrogen production plant is assumed to have infinite capacity.

### 3. GENERAL INSTRUCTIONS

#### 3.1. INSTALLATION

The simulator software is available as an executable installer. The installer will install the application needed to enable user to run the nuclear-wind HES part-task simulator. A “.zip” file is provided, which can be uploaded to any folder or directly to the desired location. The user can create the shortcut of the launcher (.exe file) to the desired location.

#### 3.2. START UP

Once the part-task simulator is installed, and shortcut created, follow these steps:

- Double click on the simulator’s launcher, “HES.exe”, to start the simulator;
- Part-task simulator home page will appear as shown in FIG. 4;
- Click on the “Start” button;
- Part-task simulator is now ready, as shown in FIG. 5;
- The user can select the mode to practice the exercises of which some are discussed in Section 4.



FIG. 4. Nuclear-wind HES part-task simulator: home page.



FIG. 5. Nuclear-wind HES part-task simulator: modes.

### 3.3. MODES

Nuclear-wind part-task simulator provides two modes: *simulator* mode and *test SMR* mode. Descriptions of these modes is provided in the following sections.

#### 3.3.1. Simulator mode

The simulator mode is used to study the instantaneous response of the HES for given rated capacities of the wind farm and the SMR by discretely varying wind speed and required load at the grid. Corresponding to these inputs, the HES response can be observed in both graphical and numerical format. The following steps are to be followed:

- Click on the “Simulator” button (FIG. 5);
- Simulator mode will start (FIG. 6) with some default inputs and corresponding outputs;
- On the screen, the user can change the rated capacities of the wind farm and SMR in the input fields (FIG. 6);
- The user can now observe the HES response by varying the wind speed or the required load using the sliders (Fig. 6). The step size for the wind speed slider is 1 m/s and for the load is 50 MWe.

Once the inputs are varied using the slider, two graphs presenting the HES response are displayed as shown in FIG. 7. The lines represent required load (reference), electrical output from SMR, electrical output from the wind farm, and total electrical output of the HES. One graph presents the data calculated without consideration of hydrogen production and the other one presents the data with hydrogen production included in calculations. With every change of

the value from slider, the calculation is performed and shown on the graphs in the form of counts.

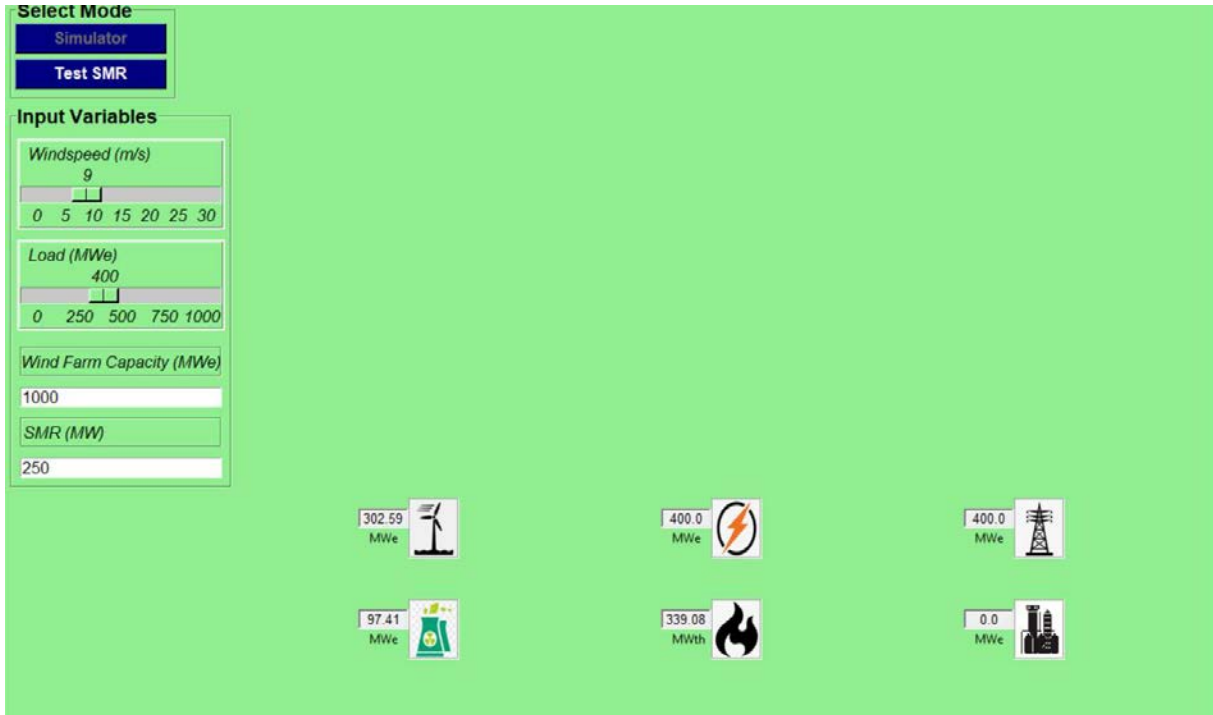


FIG. 6. Nuclear-wind HES part-task simulator: simulator mode initiation.

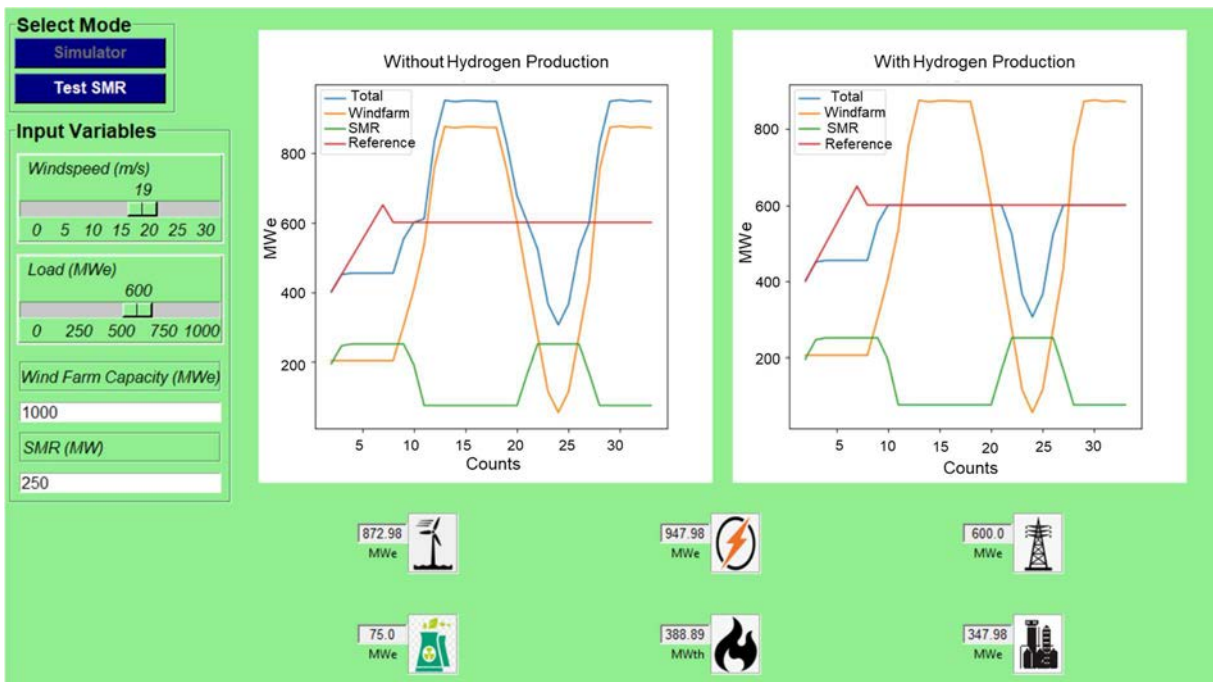


FIG. 7. Nuclear-wind HES part-task simulator: simulator mode output values.

Every change from slider represents one count on  $x$  axis which is useful for comparison of multiple inputs in a graphical way. The  $y$  axis represents electrical outputs in MWe. In the HES, hydrogen production acts as a buffer by consuming the excess electricity being produced, which

is used to perform low temperature electrolysis and thus improving load following. To study the role of hydrogen production plant, two separate graphs are provided in the simulator mode: one without hydrogen production and the second one with hydrogen production, as shown in FIG. 7. The numerical values adjacent to the icons show the HES response corresponding to the input parameters whereas the graphs show the history on how the HES response varied while changing the input parameters.

### 3.3.2. Test SMR mode

This mode requires two data sets: year-long hourly wind speed data and year-long hourly load data in addition to data required in the input fields as shown in FIG. 8. The required input values are rated capacities of SMR and windfarm, biomass quantity, and some specific values related to biomass processing (as illustrated with the screen shot shown in FIG. 9). This mode not only allows the user to observe the hourly response of the HES for any specific hour (as shown in FIG. 10) but also gives summarized calculations in the form of a schematic as illustrated in FIG. 11. To run the test SMR mode, follow the steps:

- Click on the “Test SMR” button shown on the top left corner (FIG. 8);
- Test SMR mode will start with some default inputs and outputs;
- On the screen, an input palette is provided where the user can enter the inputs required for biomass processing, the rated capacities of the wind farm, and SMR;
- Two separate buttons are provided where the year-long hourly wind speed data file and load data files can be uploaded in .txt format (FIG. 9). As an example, a wind speed data file, “windjhimpir.txt”, and a load data file, “load.txt”, are provided;
- After loading these files, the results can be seen by clicking on the “Plot” button;
- Two separate graphs, one without hydrogen production and the other with hydrogen production are displayed (FIG. 10);
- The user can observe HES response at any hour of the year using the “Hours of the year” slider (FIG. 10);
- The user can also zoom-in these two graphs using the “Span” slider (FIG. 10);
- The  $x$  axes of the graphs represent the hours of the year (with maximum limit as total number of hours for all the days of the year) having the value selected using “Hours of the Year” slider exactly in the centre of  $x$  axis. The number of hours shown in the  $x$  axes are controlled by the value selected using the “Span” slider;
- The  $y$  axes represent required load at the grid, electrical output from SMR, electrical output from the wind farm, and total electrical output of the HES in MWe.

By clicking “Schematic” (FIG. 10), HES schematics is obtained (FIG. 11) with data on:

- Total dry matter (biomass) available;
- Total thermal energy required for torrefaction;
- Total thermal energy required for pyrolysis;
- Total hydrogen produced using excess electricity;
- Remaining bio-oil;

- Per day production of biodiesel and biogasoline on an average basis. A window is provided displaying the remaining biomass, excess thermal energy, excess hydrogen produced, or deficit in hydrogen production. The “Plot” button is to be used every time, to change the input parameters.

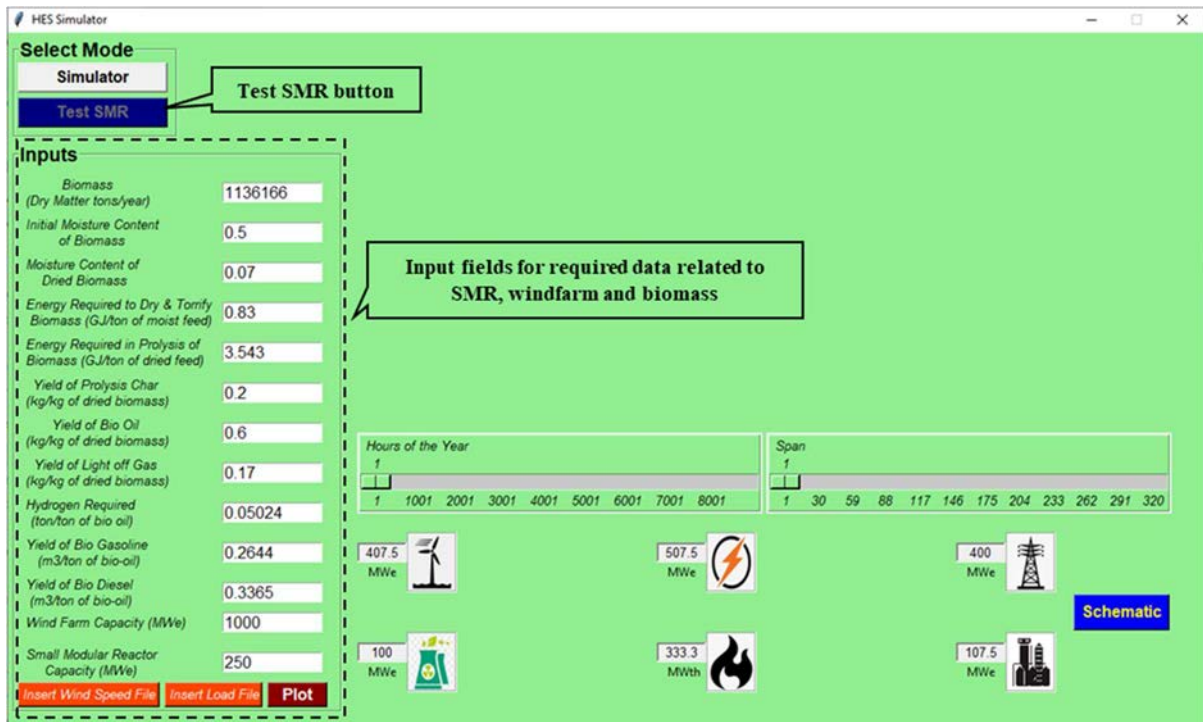


FIG. 8. Nuclear-wind HES part-task simulator: test SMR mode initiation.

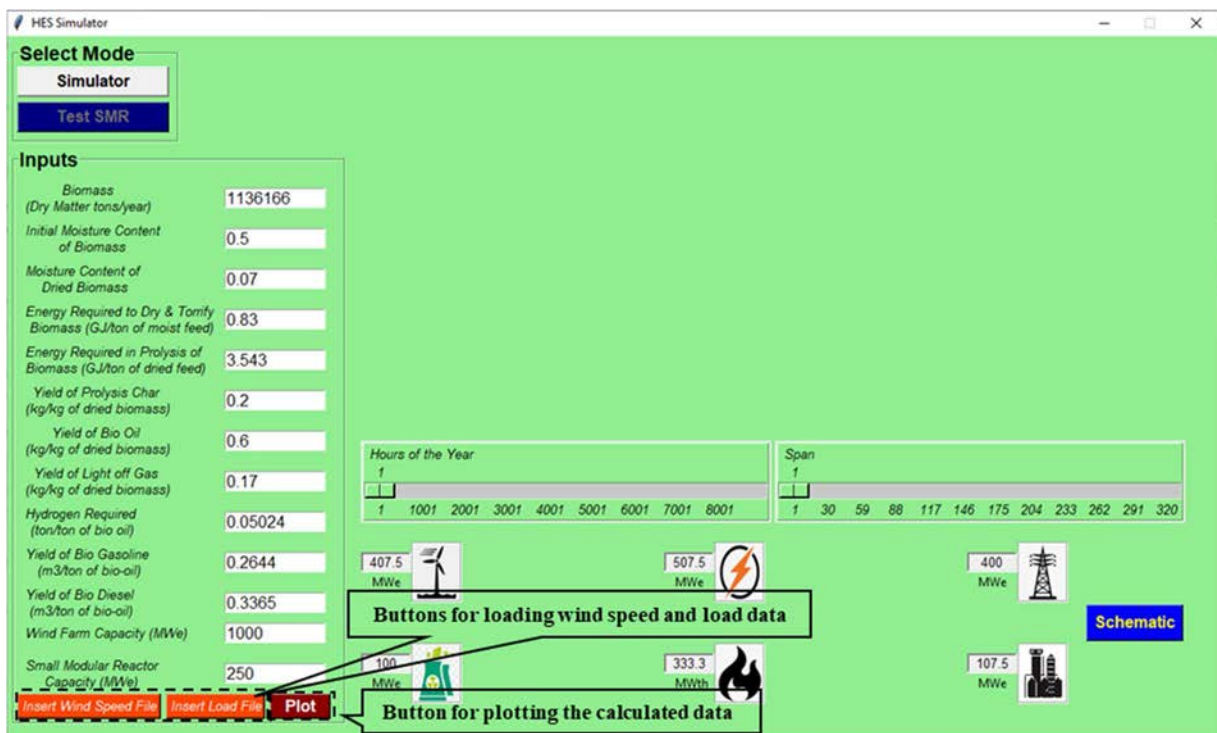


FIG. 9. Nuclear-wind HES part-task simulator: test SMR mode input data.

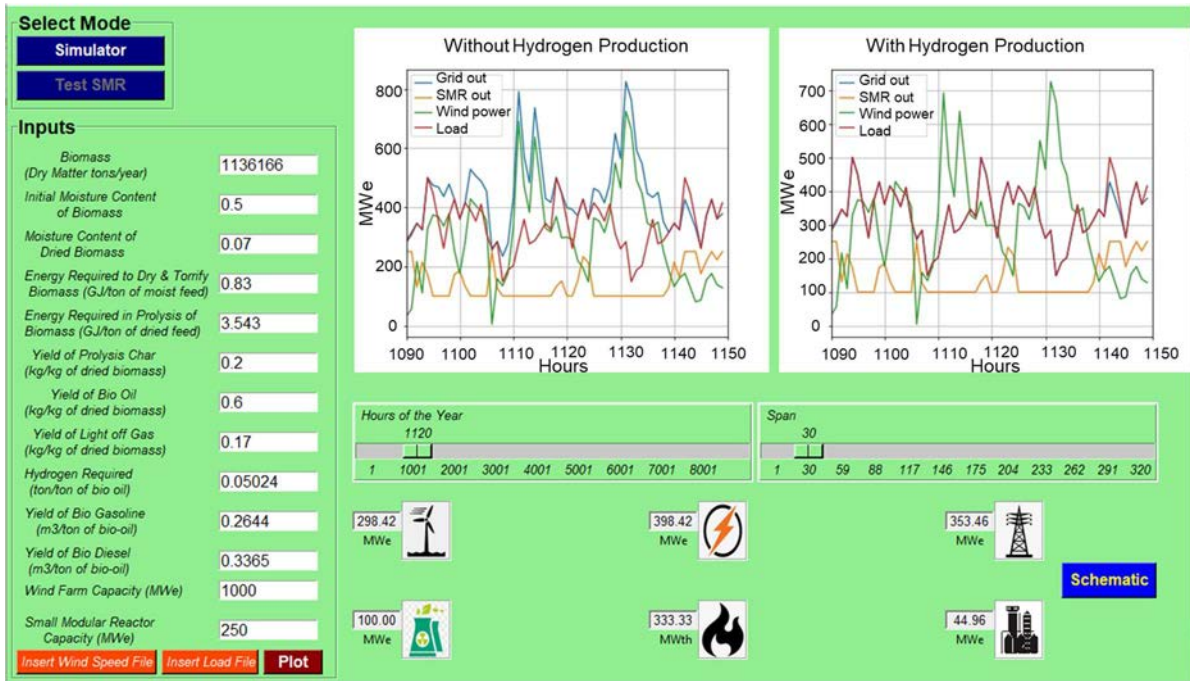


FIG. 10. Nuclear-wind HES part-task simulator: test SMR mode outputs.

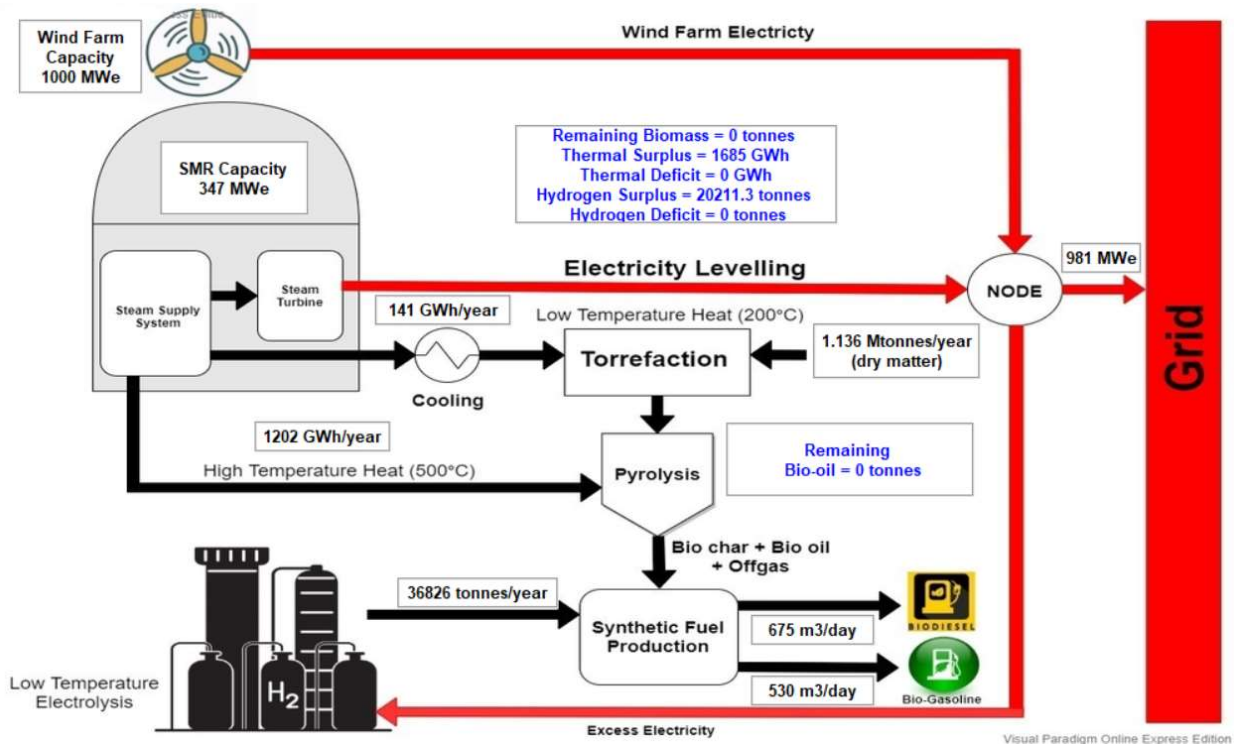


FIG. 11. Nuclear-wind HES part-task simulator: test SMR mode schematics.

#### 4. EXAMPLES

All the figures in this publication are screen shots of the simulator display and corresponding plots generated by the nuclear-wind part-task simulator. The following are examples workable for self-learning and to be used in education and training workshops and training courses.



The following sections provide descriptions of the following examples:

- Instantaneous wind speed and load;
- Yearly wind speed and load using;
- Variable biomass and energy requirements for processing;
- Effect of initial moisture content on thermal energy utilization for biomass processing;
- Effect of hydrogen requirement on synthetic fuel production.

#### 4.1. INSTANANEOUS WIND SPEED AND LOAD (SIMULATOR MODE)

FIG. 12 shows the energy flow for this example. The solid lines represent the flow of electrical energy, whereas the dashed line represents the flow of thermal energy. This example provides two scenarios to study the effect of instantaneous wind speed and load on energy distribution in the HES: input wind speed is varied instantaneously at constant load requirement as represented by case ‘a’ in FIG. 12,. and for constant input wind speed the load requirement is varied as represented by case ‘b’ FIG. 12.

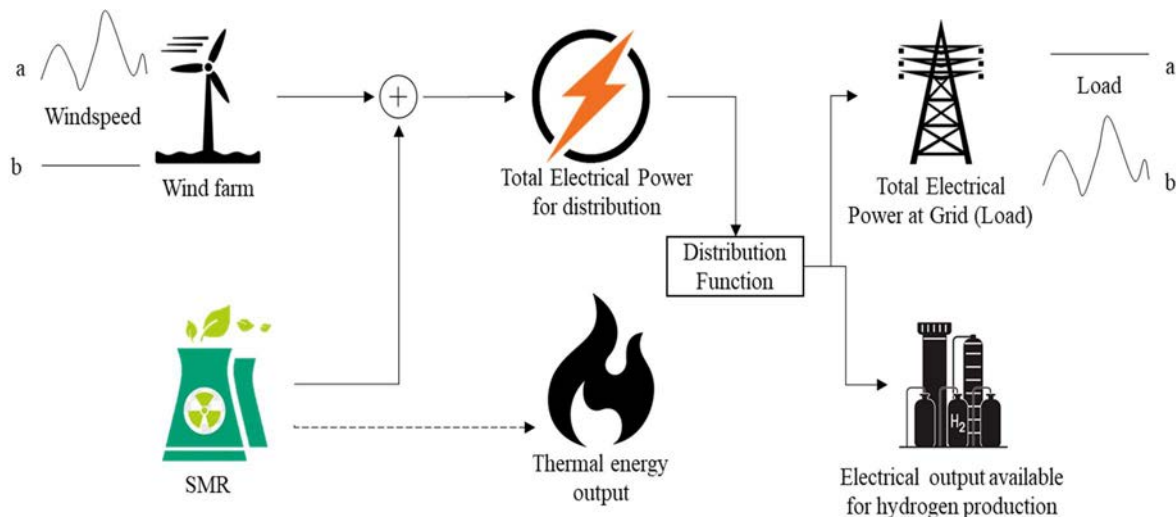


FIG. 12. Nuclear-wind HES part-task simulator: energy flow describing the example of the instantaneous wind speed and load (simulator mode).

##### 4.1.1. Simulation steps

As described in Section 3.3, in Step 1, run the nuclear-wind part-task simulator by clicking the ‘Start’ button and wait until the simulator is initialized. In Step 2, select the ‘Simulator’ button under the select mode heading. This will open the simulator mode with initially specified input values and calculated outputs as shown in FIG. 6. In Step 3, click and drag the wind speed slider moving it slowly from 9 m/s to 30 m/s with an increment of 1 m/s which will update the graphs (as shown in FIG. 13 and discussed in the following section). In Step 4, click and drag the load slider from 400 MWe to 0 MWe with decrement of 50 MWe which will update the graph (shown FIG. 14 and discussed in the following section).

#### 4.1.2. Analysis of the output parameters

FIG. 6 shows the initial values as follows: wind speed is 9 m/s, load requirement of 400 MWe, wind farm capacity is set to 1,000 MWe and the SMR rated capacity is 250 MWe. The power output from the wind farm is calculated from FIG. 2 based on specified windspeed which gives 302.6 MWe. The initial load requirement (reference) is higher than the electrical power output from the wind farm. The difference between the load requirement and the electrical power output from wind farm is 97.4 MWe, which is greater than 30% of the SMR electrical power output (i.e., 75 MWe). This difference (i.e., 97.4 MWe) is provided by the SMR, as the electrical power output of the SMR can be varied between 30% and 100%. The remaining power output (339MWth) from the SMR is used to fulfill the thermal energy requirement for biomass processing. The total electrical power output available from HES is 400 MWe, which is completely utilized to meet the load demand. The electrical power output available for hydrogen production is zero.

FIG. 13 shows the wind speed increased from 9 m/s to 30 m/s. The load requirement is kept at constant value of 400 MWe, which is shown in the graphs as 'Reference'. The electrical power obtained from the wind farm increases initially with increasing wind speed and exceeds the load requirement. The SMR is operated at 30% of its capacity (i.e. at 75 MWe) when the electrical power from the wind farm is higher than the load requirement. The excess thermal energy from SMR is used for biomass processing and the excess electrical power output is used for hydrogen production. The graph on the left hand side of Fig. 13 shows the 'Total' electrical power available at the grid if hydrogen production facility is not utilized, whereas the graph on the right hand side of this same figure, shows 'Total' electrical power at the grid that overlaps with the 'Reference' as the excess electricity is utilized for hydrogen production. At the very high wind speed the electrical power output from the wind farm falls below the load requirement, so the SMR is switched to 100% electrical power output and provides 250 MWe. The electrical power from the wind farm is 56 MWe when the SMR is operating at 100% capacity. The total electrical power output at the grid is 306 MWe which is less than the load requirement (400 MWe). Therefore, in this case total power available for distribution is used at the grid and zero power is available for both biomass processing and hydrogen production.

FIG. 14 shows the extension of information contained in FIG. 13, when load requirement at the grid is reduced from 400 MWe to 0 MWe at a constant wind speed of 30 m/s. The graphs show that as the load requirement decreases below 306 MWe, the SMR electrical power output starts to decrease from 100% to 30%. When the load requirement reaches the zero value, the SMR is operating at the lowest electrical power output (30% capacity i.e., 75 MWe). The wind farm is producing 56 MWe and the total electrical power available for distribution is 131 MWe. Since the load requirement at this point is zero, the total electrical power available of 131 MWe is utilized for hydrogen production. The excess thermal power from SMR of 389 MWth is utilized for biomass processing.

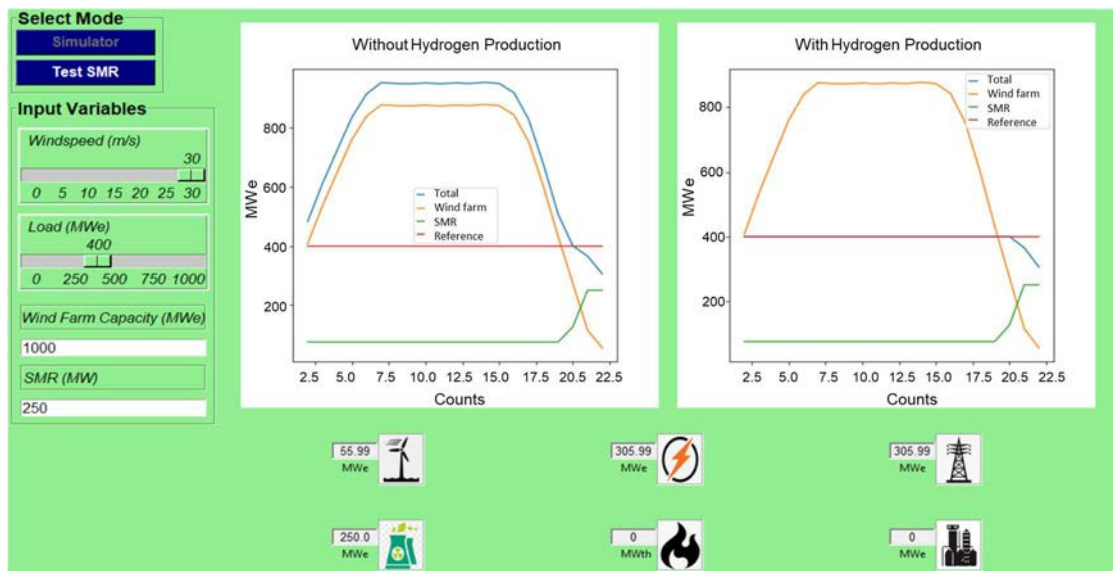


FIG. 13. Nuclear-wind part HES task simulator: output variables in the example of the instantaneous wind speed variation (simulator mode).

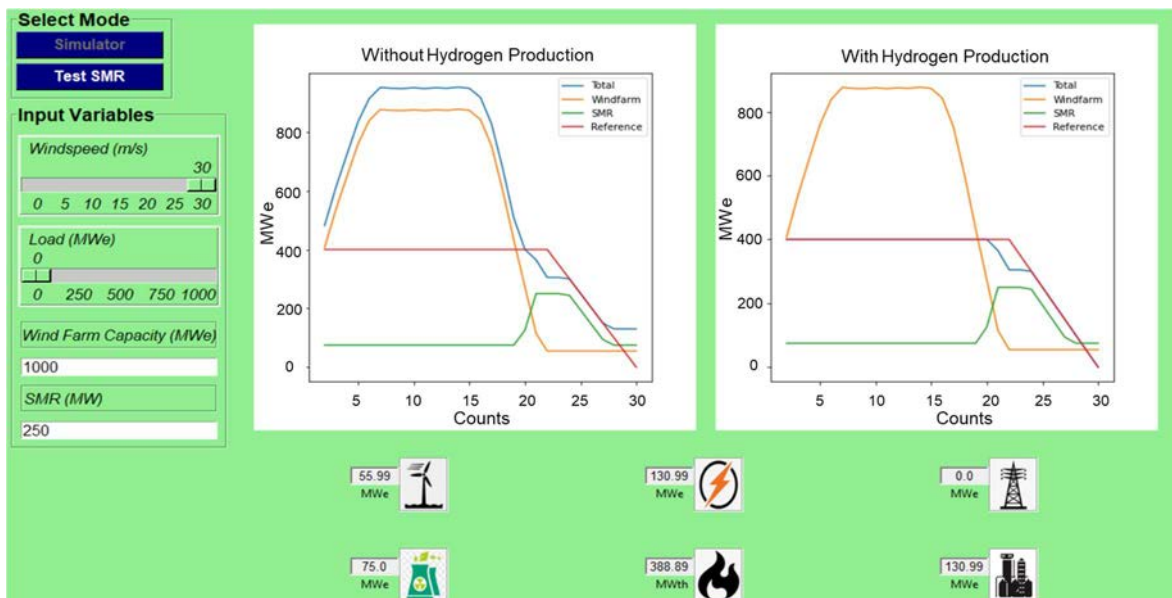


FIG. 14. Nuclear-wind HES part task simulator: output values in the example of the instantaneous load variation (simulator mode).

#### 4.2. YEARLY WIND SPEED AND LOAD DATA (TEST SMR MODE)

The ‘Test SMR’ mode is to be selected when using yearly windspeed and load to calculate the hourly net electrical power to grid, thermal energy utilization and hydrogen production, as well as yearly average for total hydrogen production, biodiesel, biogasoline, hydrogen surplus, hydrogen deficit, thermal surplus, thermal deficit, and the remaining biomass.

FIG. 15 shows the energy and material flow for this example. The solid lines represent the electrical energy, the dashed lines represent the thermal energy and the dotted line represent the flow of materials. In this example, the output parameters for the biomass processing and the

flow of energy for nuclear-wind HES are studied for yearly variation of both the wind speed and load requirement as represented with ‘a’ in FIG. 15.

The thermal energy available from the SMR and the hydrogen produced, are both utilized in biomass processing plant. Detailed model flow of energy and material inside the biomass processing plant is shown in FIG. 3.

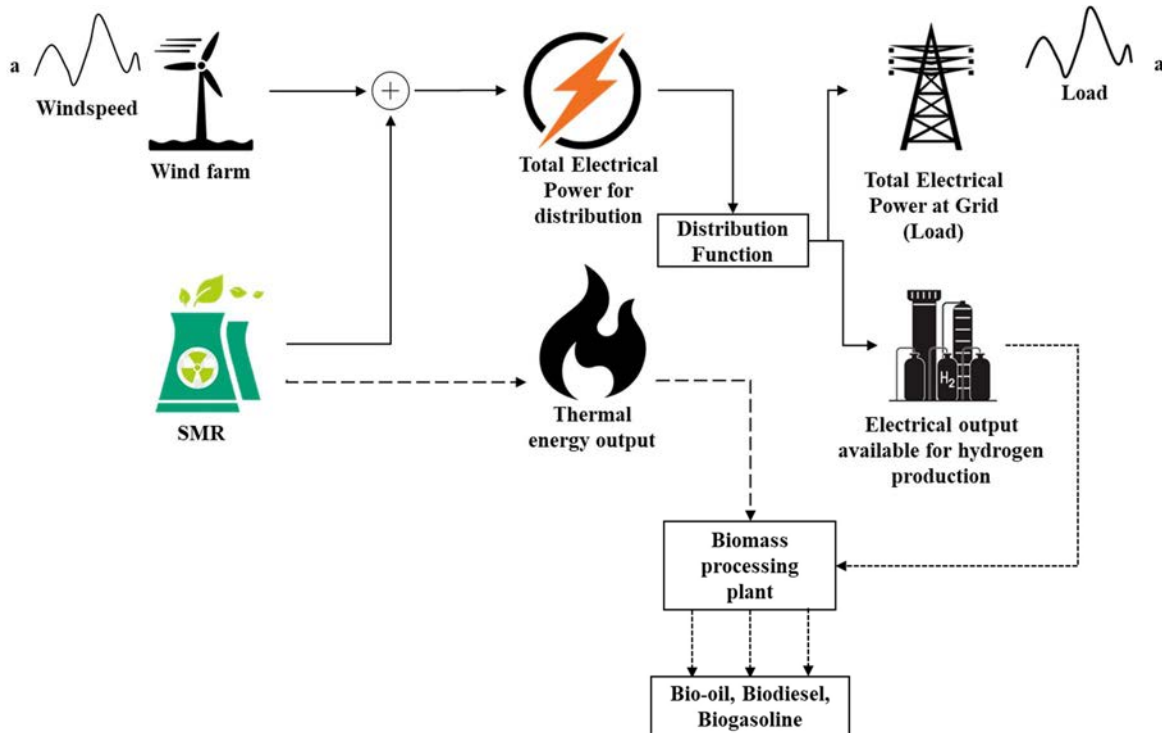


FIG. 15. Nuclear-wind HES part-task simulator: energy and material flow describing the example of yearly wind speed and load (test SMR mode).

The hourly data for load and windfarm output power are taken from [12] as shown in FIG. 16; it is assumed that the same cycle for wind farm output power and load is repeated every month. The nuclear-wind part-task simulator uses the wind speed as an input instead of wind farm output power, so the respective values of wind speed are used for the analysis from FIG. 2. FIG. 16 also shows hourly variation of the output parameters such as reactor power, power to grid from HES and the electrical output power for H<sub>2</sub> production. Whenever the wind farm output power exceeds the load value, the reactor power is shifted to minimum and power to grid from HES follows the load curve.

The maximum number of peaks for wind farm output power occurs near the mid of the month. Similar trend for reactor power and power to grid from HES can be obtained using the nuclear-wind part-task simulator. Moreover, the instantaneous value of all output parameters at any hour of the year can also be noted and compared with the data from FIG. 16 (as discussed in Section 4.2.2).

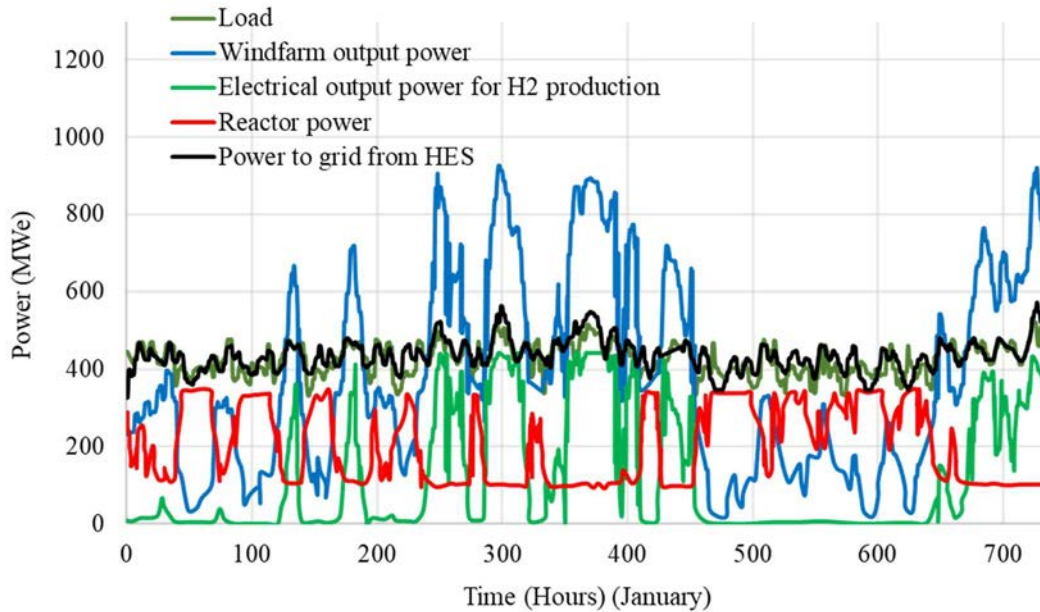


FIG. 16. Hourly power data for a nuclear-wind HES.

#### 4.2.1. Simulation steps

As described in Section 3.3, in Step 1, run the nuclear-wind part-task simulator by clicking the ‘Start’ button and wait until the simulator is initialized. In Step 2, select the ‘Test SMR’ mode. This will open the simulator in ‘Test SMR’ mode as shown in FIG. 8. In Step 3, change the value of SMR capacity from 250 MWe to 347 MWe, and wind farm capacity from 1,000 MWe to 1,018 MWe. The details of the remaining input parameters are shown in FIG. 17. All these parameters are set by default in the part-task simulator. In Step 4, select the ‘Insert Wind Speed File’ button, and select the ‘WindSpeedforValidation.txt’ file. In Step 5, click the ‘Insert Load Speed File’ button, and select the ‘LoadforValidation.txt’ file. In Step 6, click on ‘Plot’ button and wait until the calculations are complete. When the calculations are complete the data is available for visualization. In Step 7, click and drag the ‘Span’ slider to 360. In Step 8, click and drag the ‘Hours of the Year’ slider to 382 to view the results for the first month of the year as shown in FIG. 17 and discussed in the following section. In Step 9, click on the ‘Schematic’ button to view the yearly details for hydrogen production and biomass processing as shown in FIG. 18.

#### 4.2.2. Analysis of the output parameters

The graph on the left hand side in FIG. 17, represents the load, SMR electrical power (SMR Out), wind farm electrical power (Wind Power) and electrical power available at the grid without hydrogen production (Grid Out) whereas the graph on the right represents the load, SMR electrical power (SMR Out), wind farm electrical power (Wind Power) and electrical power available at the grid with hydrogen production (Grid Out). The graph on the right is similar to the one obtained from the [12] as shown in FIG. 16. The ‘Grid Out’ (shown as ‘Power to grid from HES’) exactly follows the ‘Load’ curve without any delay when hydrogen production is utilized, but in reality there is always a small difference as shown in the actual

data as shown in FIG. 16. The icons below the graphs represent the instantaneous value of the output parameters at 382<sup>nd</sup> hour of the year. At this hour, the load is 467.2 MWe, whereas the windfarm is producing the 880.9 MWe which is higher than the load value. So, the SMR is operating at 30% capacity i.e., 104.1 MWe. The remaining 539.8 MWth thermal energy from the SMR is used for biomass processing. The total electrical power available for distribution at the node is 985 MWe out of which 467.2 MWe is used to meet the load demand and the remaining 517.8 MWe is used for hydrogen production.

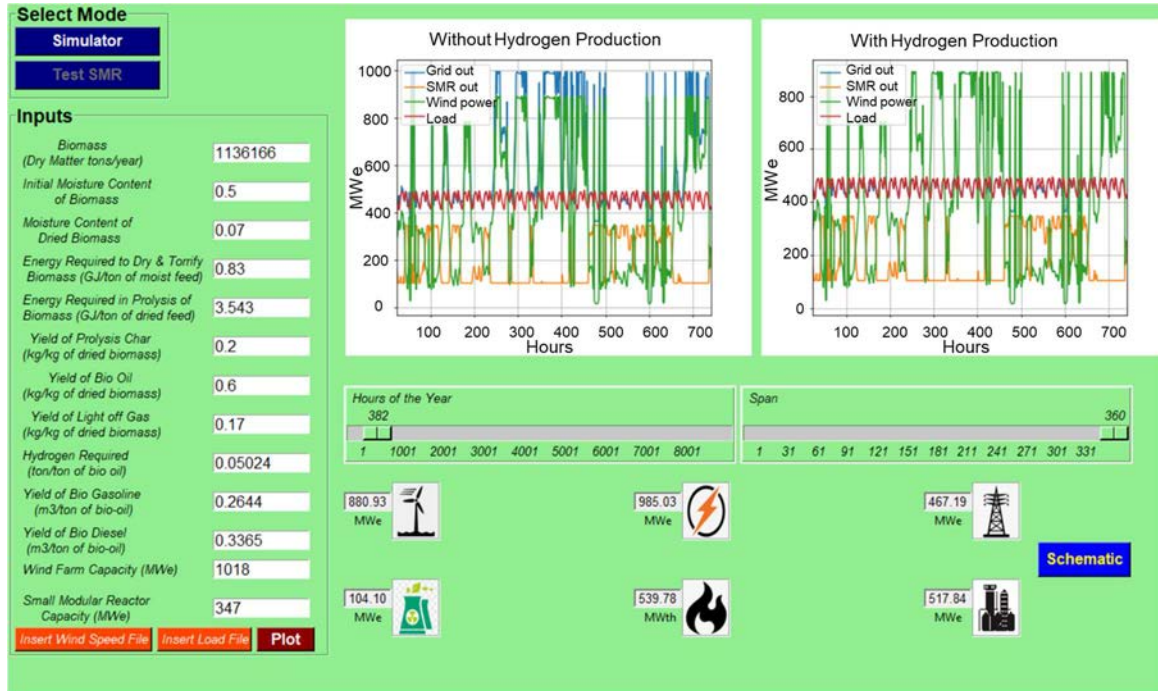


FIG. 17. Nuclear-wind HES part task simulator: output values in the example of yearly wind speed and load data (test SMR mode).

FIG. 18 shows the yearly details of biomass processing output parameters. The total energy required per year for torrefaction is 141 GWh, whereas the total energy required per year for pyrolysis 1,202 GWh. The total hydrogen utilized per year for bio-oil processing is 36,826 tonnes. There is thermal surplus of 1,716 GWh and hydrogen surplus of 22,416 tonnes, which shows that all the biomass initially available is converted to synthetic fuel.

The data obtained for biomass processing from the schematics (FIG. 18) and the energy distribution from HES (FIG. 17) is summarized in TABLE 1 for the 382<sup>nd</sup> hour of the year and compared to data from [12]. The maximum difference of 14% is observed due to the following reasons:

- Only data for January was available in the reference, which was repeatedly used in this example for every other month in a year;
- It was assumed that the reactor will follow the load without any delay but in real scenario, nuclear reactor takes time (lag) in following the electricity demand which causes errors in electricity outputs obtained through part-task simulator.

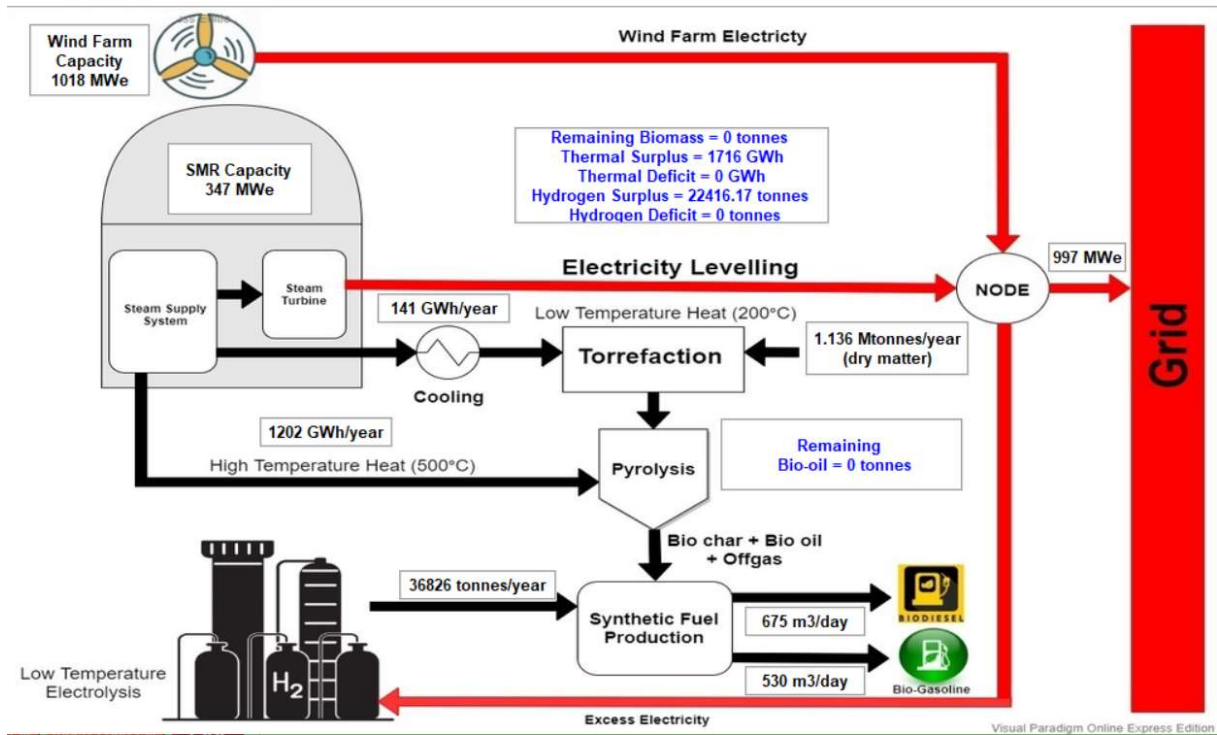


FIG. 18. Nuclear-wind HES part task simulator: details of biomass and hydrogen production in the example of yearly wind speed and load data (test SMR mode).

TABLE 1. COMPARISON OF PART-TASK SIMULATOR VALUES WITH REFERENCE DATA [12]

Parameter	Nuclear-Wind HES Part-Task Simulator	Values from Ref. [12]	Difference (%)
Reactor output (MWe)	104.1	104.1	0
Power to grid (MWe)	467.2	540	13
Electricity for H <sub>2</sub> production (MWe)	517.8	453	14
Hydrogen used for oil treatment (kT)	36.8	42	12
Biogasoline production (m <sup>3</sup> /day)	530	597	11
Biodiesel production (m <sup>3</sup> /day)	675	753	10

#### 4.3. VARIABLE BIOMASS AND ENERGY REQUIREMENTS FOR PROCESSING

In this example the input parameters related to the biomass processing are changed keeping all other parameters same as those described in Section 4.2. This will not affect the electrical outputs at the grid because the input power from the wind farm and the load requirement are the same.

##### 4.3.1. Simulation steps

This simulation follows the same steps as described in Section 4.2.1. The difference is in Step 3, in which to replace the ‘biomass’ value with 11,361,660 which is ten times higher. Then follow the steps described in Section 4.2.1. The results obtained for biomass processing are shown in FIG. 19. In the next step, close the schematic window and change the ‘Energy Required to Dry and Torrify Biomass’ to 0.1, and ‘Energy Required in Pyrolysis of Biomass’

to 0.5. Click on the ‘Plot’ and then ‘Schematic’ to view the results (as shown in FIG. 20 and discussed in the following section).

#### 4.3.2. Analysis of the output parameters

FIG. 19. Nuclear-wind HES part task simulator: output values shows schematics of a biomass processing and hydrogen production when dried biomass value is changed from 1.1 Mt/year to 11 Mt/year. There is a large amount of remaining biomass i.e., 8.8 Mt, which does not undergo torrefaction because of insufficient thermal power available throughout the year. The total thermal deficit is 10,374 GWh. The thermal energy required for torrefaction of biomass is 1,410 GWh/year, whereas the thermal energy required for pyrolysis is 12,024 GWh/year. There is also a hydrogen deficit of 24,636 tonnes, which shows that electrical power available for hydrogen production throughout the year is not enough for complete conversion of bio-oil to synthetic fuel. Thus, 490,374 tonnes of bio-oil are available at the output of the biomass processing plant. The synthetic fuel produced from the biomass processing plant contains biodiesel and biogasoline. Daily production of biodiesel and biogasoline is 1,087 m<sup>3</sup>/day and 854 m<sup>3</sup>/day, respectively.

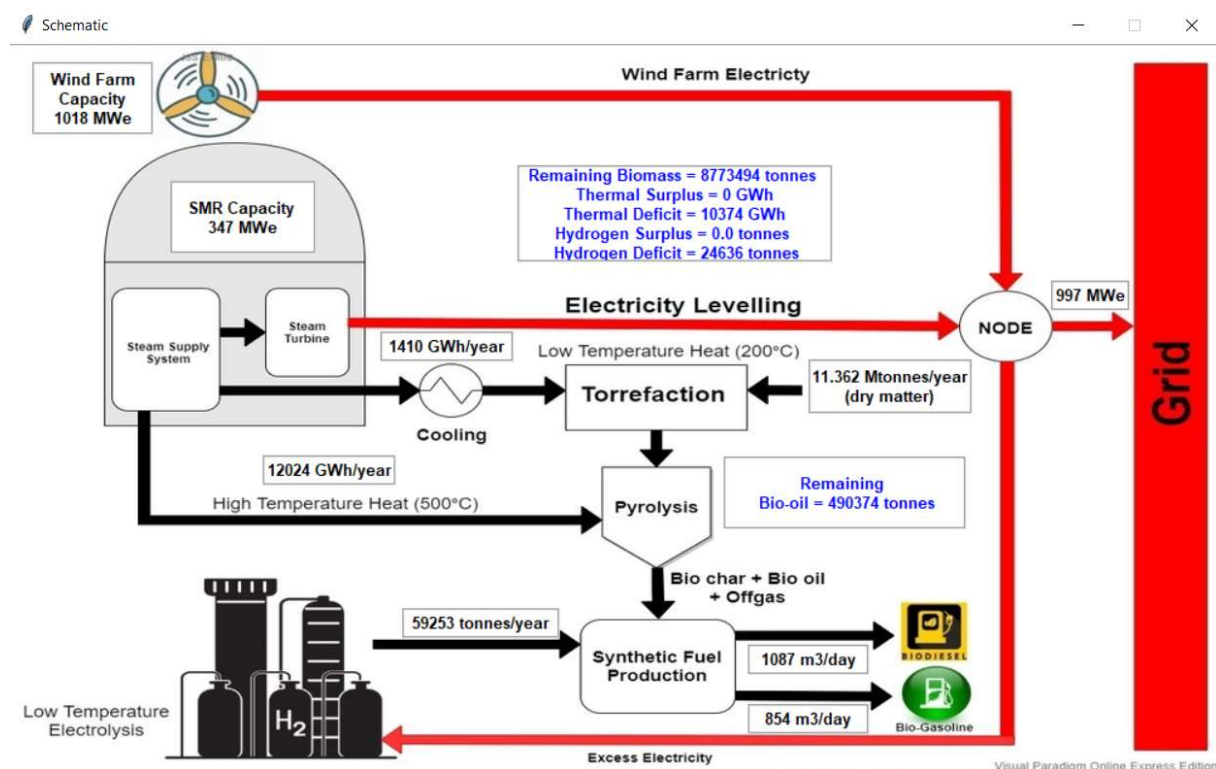


FIG. 19. Nuclear-wind HES part task simulator: output values for variable dried biomass in the example of variable biomass and energy requirements for biomass processing (test SMR mode).

FIG. 20. Nuclear-wind HES part task simulator: shows schematics of a biomass processing and hydrogen production with the assumption that relatively small amount of thermal power is required for torrefaction and pyrolysis. In this case, total energy required for torrefaction is 169 GWh and the energy required for pyrolysis is 1,696 GWh. The thermal surplus of 1,193 GWh shows that thermal energy from SMR during the year is sufficient to convert all biomass into



its byproduct i.e., bio-oil. The total thermal energy produced during a period of one year is the algebraic sum of thermal surplus, energy required for drying and torrefaction, and the energy required for pyrolysis minus thermal deficit, which is 3,059 GWh/year. There also exists a hydrogen deficiency of 309,010 tonnes, therefore the bio-oil produced from pyrolysis is not completely converted into synthetic fuel. The remaining bio-oil of 6,150,693 tonnes is available as the output from the biomass processing plant.

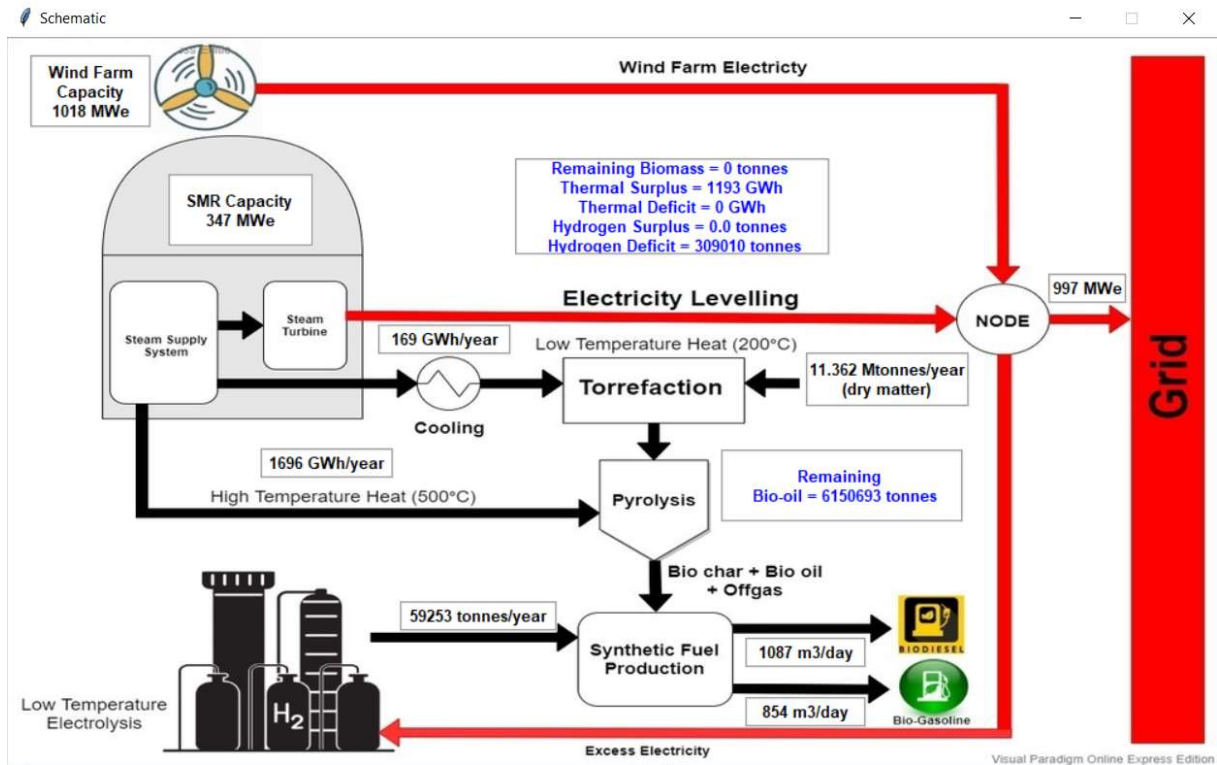


FIG. 20. Nuclear-wind HES part task simulator: output values for variable energy requirements in the example of variable biomass and energy requirements for biomass processing (test SMR mode).

#### 4.4. EFFECT OF INITIAL MOISTURE CONTENT ON THERMAL ENERGY UTILIZATION FOR BIOMASS PROCESSING (SMR MODE)

This example is the extension of example described in Section 4.3. In this example the initial moisture content of the biomass is varied to study the effect on thermal energy utilized for drying and torrefaction of biomass.

##### 4.4.1. Simulation steps

This example follows the same simulation steps as described in Section 4.3.1. with changing the 'Initial Moisture Content of Biomass' to 0.1. Then click on 'Plot' button to run the example as shown in FIG. 21. Then click on 'Schematic' button to view the results as shown in FIG. 22. Repeat the simulation steps with 'Initial Moisture Content of Biomass' varying from 0.1 to 0.9 with increment of 0.1 and record the energy required for drying and torrefaction and thermal surplus as shown in TABLE 2.

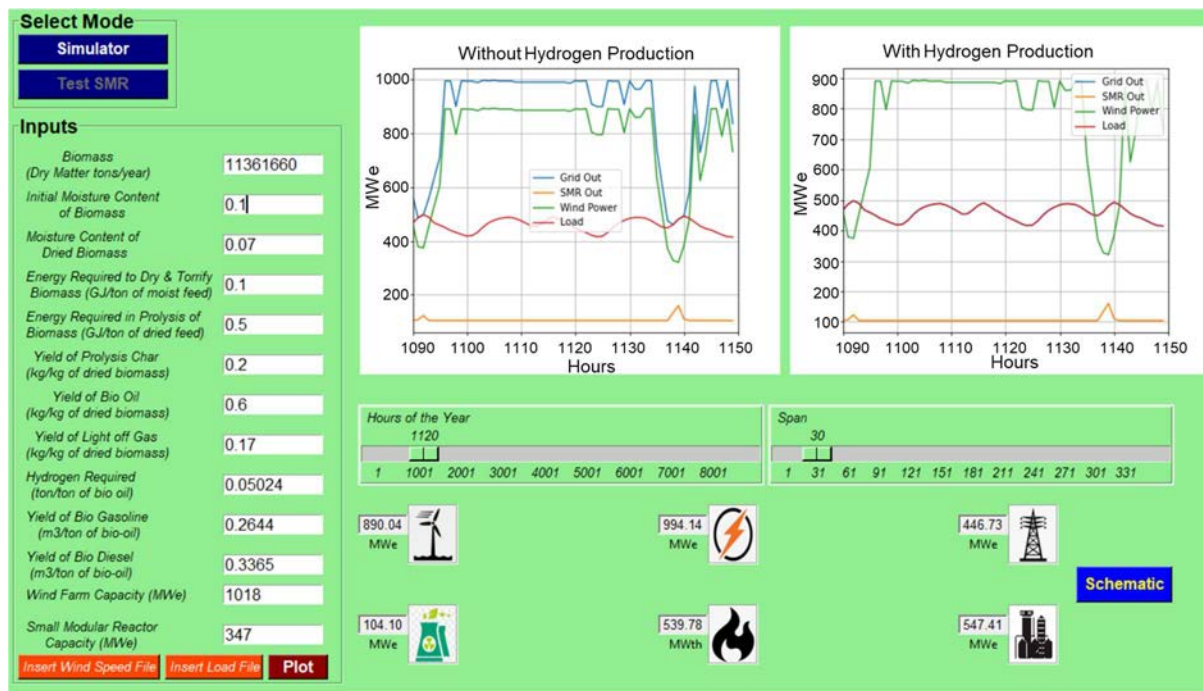


FIG. 21. Nuclear-wind HES part task simulator: input parameters in the example of the effect of initial moisture content on thermal energy requirement for biomass processing (test SMR mode).

#### 4.4.2. Analysis of the output parameters

FIG. 22 shows schematics of biomass processing and hydrogen production at initial moisture content of 0.1. All output parameters are as shown in FIG. 20, except that thermal surplus is 1,269 GWh and energy required for drying and torrefaction is 94 GWh/year. The energy required for pyrolysis of the biomass is 1,696 GWh/year. Total thermal energy produced in one year is 3,059 GWh, which is the same as in example described in Section 4.3.2, because of the same load requirements, wind farm output power and SMR output power. TABLE 2 shows the energy required for drying and torrefaction with thermal surplus as the initial moisture content of biomass varied between 0.1–0.9. The energy required for drying and torrefaction increases exponentially from 94 GWh/year to 849 GWh/year with increase of initial moisture content. Thermal surplus decreases by same amount showing that thermal energy is used for biomass processing.

TABLE 2. VARIATION OF ENERGY UTILIZATION FOR BIOMASS PROCESSING WITH INITIAL MOISTURE CONTENT

Initial Moisture Content of the Biomass	Energy Required for Drying and Torrefaction (GWh/year)	Thermal Surplus (GWh/year)
0.1	94	1,269
0.2	106	1,257
0.3	121	1,242
0.4	141	1,221
0.5	169	1,193
0.6	212	1,151
0.7	283	1,080
0.8	424	938
0.9	849	513

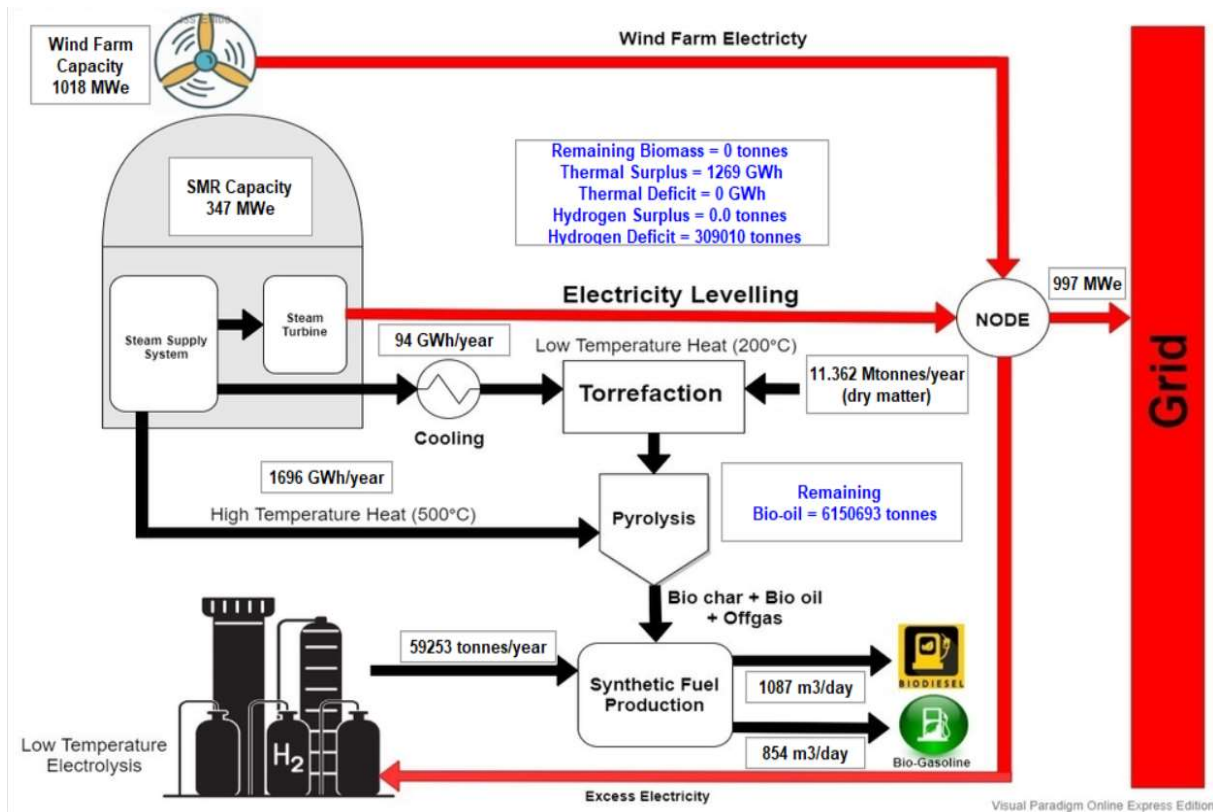


FIG. 22. Nuclear-wind HES part task simulator: output parameters in the example of the effect of initial moisture content on thermal energy requirement for biomass processing (test SMR mode).

#### 4.5. EFFECT OF HYDROGEN REQUIREMENT ON SYNTHETIC FUEL PRODUCTION (SMR MODE)

In this example, the effect of hydrogen required per tonne of bio-oil on hydrogen utilized for synthetic fuel production is studied by keeping all other parameters constant.

##### 4.5.1. Simulation steps

This simulation follows the same steps as described in Section 4.2.1. The only difference is in Step 3, in which the 'Hydrogen required ton/ton of bio-oil' is set to 0.06, as shown in FIG. 23. Details of the biomass processing parameters obtained from the simulation are shown in FIG. 24. In the next Step, change the 'Hydrogen required ton/ton of bio-oil' from 0.07 to 0.10 with the increment of 0.01, and record the hydrogen surplus and hydrogen utilized per year for the conversion of biomass to synthetic fuel as shown in TABLE 3.

##### 4.5.2. Analysis of the output parameters

FIG. 24 shows schematics of biomass processing output parameters for 0.06 tonne of hydrogen required per tonne of bio-oil. The hydrogen surplus is 15,250 tonne, while hydrogen utilized during period of one year under specified wind power and load conditions is 43,980 tonne. Total hydrogen produced during a period of one year is the sum of hydrogen surplus and hydrogen utilized, which is 59,230 tonne. Changing the hydrogen required per tonne of bio-oil

affects the hydrogen surplus, hydrogen deficit and hydrogen utilized for synthetic fuel production.

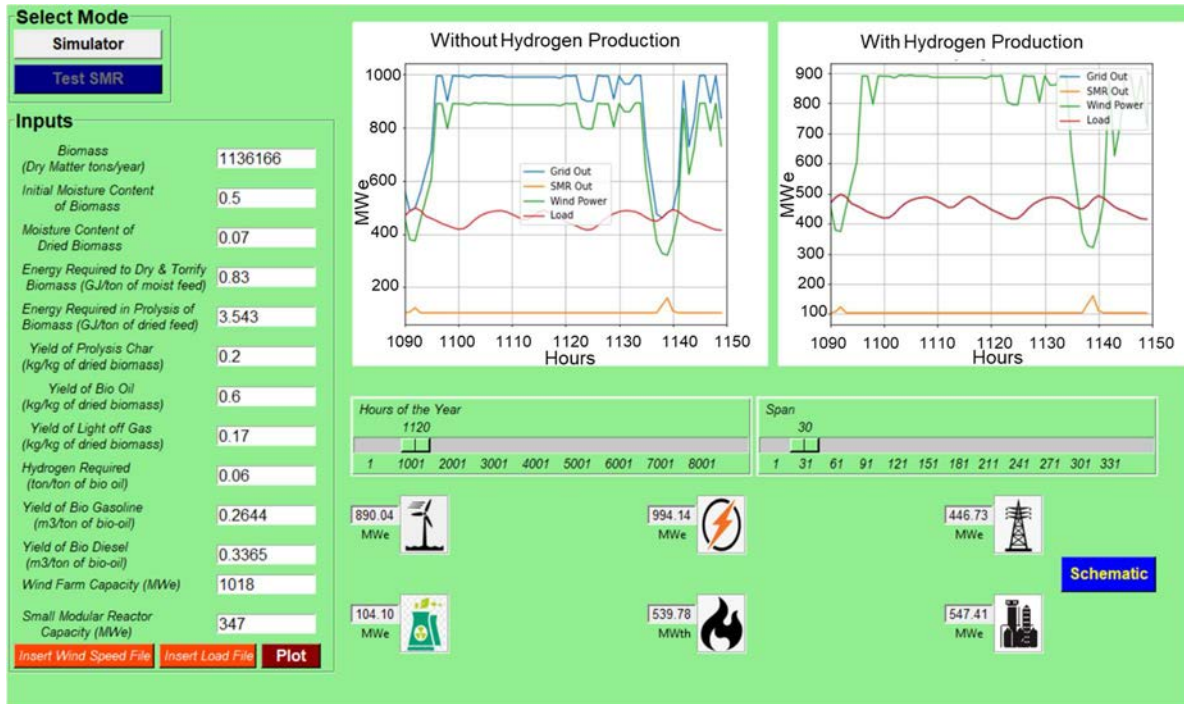


FIG. 23. Nuclear-wind HES part task simulator: input parameters in the example of the effect of hydrogen requirement on synthetic fuel production (test SMR mode).

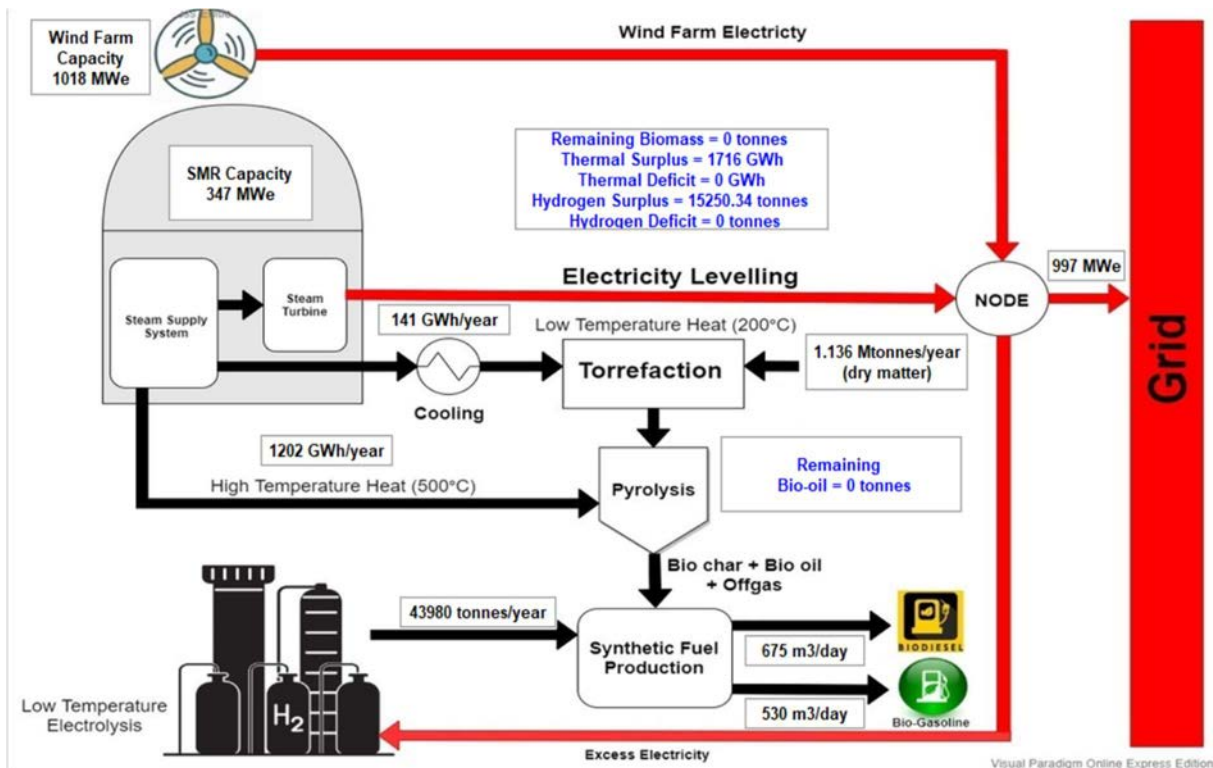


FIG. 24. Nuclear-wind HES part task simulator: output parameters in the example of the effect of hydrogen requirement on synthetic fuel production (test SMR mode).

Table 3 provides the output values obtained when hydrogen requirement per tonne of bio-oil is changed from 0.07 to 0.10. Hydrogen utilized for synthetic fuel production increases as hydrogen requirement per tonne of bio-oil is increased, until all the hydrogen produced during the year is utilized. Total hydrogen produced is completely utilized as hydrogen requirement per tonne of bio-oil exceeds 0.08. Increasing hydrogen requirement per tonne of bio-oil further increases hydrogen deficit, showing the amount of hydrogen which is required for complete conversion of bio-oil to synthetic fuel.

**TABLE 3. VARIATION OF HYDROGEN REQUIREMENTS FOR BIOMASS PROCESSING WITH HYDROGEN REQUIRED PER TONNE OF BIOMASS**

<b>Hydrogen Required per Tonne of Bio-oil</b>	<b>Hydrogen Utilized (tonne/year)</b>	<b>Hydrogen Surplus/Deficit* (tonne/year)</b>
0.07	51,310	7,900
0.08	58,640	597
0.09	59,253	-6,717
0.10	59,253	-14,047

\*Negative values represent hydrogen deficit

## REFERENCES

- [1] INTERNATIONAL ATOMIC ENERGY AGENCY, Classification, Selection and Use of Nuclear Power Plant Simulators for Education and Training, IAEA-TECDOC-1887, IAEA, Vienna (2019).
- [2] BERRADA, A. (Eds), EL MRABET, R. (Eds), Hybrid Energy System Models, Academic Press, US (2020).
- [3] INTERNATIONAL ATOMIC ENERGY AGENCY, Nuclear-Renewable Hybrid Energy Systems, IAEA-NR-T-1.24, IAEA, Vienna (2022).
- [4] NETO, M. B., CARVALHO, P. C., CARIOCA, J. O., CANAFISTULA, F., J., Biogas/photovoltaic hybrid power system for decentralized energy supply of rural areas, *ENERGY POLICY* **38** 8 (2010) 4497, 4506.
- [5] NIXON, J. D., DEY, P. K., DAVIES, P. A., The feasibility of hybrid solar biomass power plants in India, *Energy* **46** 1 (2012) 541, 554.
- [6] REHMAN, S., AL-HADHRAMI, L. M., Study of a solar PV-diesel-battery hybrid power system for a remotely located population near Rafha, Saudi Arabia, *Energy* **35** 12 (2010) 4986, 4885.
- [7] ZOUBEIDI, O. M., FARDOUN, A. A., NOURA, H., NAYAR, C., Hybrid renewable energy system solution for remote areas in UAE, *Global Journal of Technology and Optimization* **3** (2012) 115, 121.
- [8] KALDELLIS, J. K., KAVADIAS, K. A., Cost-benefit analysis of remote hybrid wind-diesel power stations: case study Aegean Sea islands, *Energy Policy* **35** 3 (2007) 1525, 1538.
- [9] RUBIO-MAYA, C., UCHE-MARCUELLO, J., MARTÍNEZ-GRACIA, A., BAYOD-RÚJULA, A. A., Design optimization of a polygeneration plant fuelled by natural gas and renewable energy sources, *Applied Energy* **88** 2 (2011) 449, 457.
- [10] BRAGG-SITTON, S. M., et al., Nuclear-Renewable Hybrid Energy Systems: 2016 Technology Development Program Plan, Idaho National Lab (INL), Rep. INL/EXT-16-38165, Idaho Falls, Oak Ridge, TN (United States) (2016).
- [11] CHERRY, R. S., AUMEIER, S. E., BOARDMAN, R. D., Large hybrid energy systems for making low CO<sub>2</sub> load-following power and synthetic fuel, *ENERGY and Environmental Science* **5** 2 (2012) 5489, 5497.
- [12] CARLSSON, J., PURVINS, A., PAPAIOANNOU, I. T., SHROPSHIRE, D., CHERRY, R. S., Conceptual Evaluation of Hybrid Energy System Comprising Wind-Biomass-Nuclear Plants for Load Balancing and for Production of Renewable Synthetic Transport Fuels, *Proceedings of the HTR 2014, China* (2014).
- [13] SHROPSHIRE D., PURVINS, A., PAPAIOANNOU, I., MASCHIO, I., Benefits and cost implications from integrating small flexible nuclear reactors with off-shore wind farms in a virtual power plant, *Energy Policy* **46** (2012) 558, 573.
- [14] BASU, P., Biomass Gasification, Pyrolysis and Torrefaction, Edn. 3, Academic Press, US (2013).
- [15] "Biomass Atlas for Pakistan," World Bank and AEBD, Pakistan (2016).
- [16] PERIYASAMY, K., PERIYASAMY, R., KARTHIKEYAN, R. N., GOPINATH, A., GOKULNATH, KARTHICKANNAN, V., Improve the efficiency of boiler by reduce the moisture in bagasse, *International Journal of Engineering Research & Technology* **6** (2018) 1, 7.
- [17] HUGO., T. J., Pyrolysis of Sugarcane Bagasse, PhD Thesis, University of Stellenbosch, South Africa (2010).

- [18] SHOAIB, Q., MUHAMMAD, A., YOUNAS, M., Fast pyrolysis of sugarcane bagasse: Effect of pyrolysis conditions on final product distribution and properties, *Energy Sources, Part A: Recovery, Utilization, and Environmental Effects* **39** 2 (2017) 184, 190.

## ANNEX I WIND FARMS

### I-1. INTRODUCTION

A wind farm is a group of wind turbines to produce electricity using kinetic energy of the wind [I-1]. The wind turbines can be either horizontal axis or vertical axis. The horizontal axis wind turbines have a physical energy conversion limit, known as the Betz's limit, according to which the maximum power potential of the horizontal axis wind turbine cannot be larger than 59.3% of the total available power. Often this limit is also applicable to vertical axis wind turbines, but the research showed that the efficiency of the vertical axis wind turbines can be higher [I-2]. Almost all wind farms in operation across the world use the horizontal axis wind turbines.

The wind farm can be either onshore or offshore. The number of wind turbines in a wind farm can vary from as few as five to hundreds, covering a very large land area. The first European wind farm had only five wind turbines of less than 11 m rotor diameters [I-3]. However, with the development of wind energy technology, the size of wind turbines as well as the total number of wind turbines in a wind farm increases rapidly. Gansu, the world largest wind farm has 7,000 turbines, each with 120 m in rotor diameter.

The total wind energy generation at the end of 2021 is 1870 TWh with 93% of the energy coming from onshore wind farms whereas the remaining 7% from the offshore wind farms [I-4]. Figure I-1 shows the details of various onshore and offshore wind farms operating across the world [I-5]. Hornsea 1 is the largest offshore windfarm in operation having capacity of 1218 MW, whereas Gansu is the largest onshore windfarm with current capacity of 8000 GW.

### I-2. DESIGN OF A WIND FARM

The design of wind farm is very complex affected by geographical, logistical, environmental, and technological factors such as but not limited to site, wind turbine placement, capacity of the wind farm, and the economic feasibility of the wind farm throughout its life span. These factors highly influence the design and the net power output of the wind farm.

In designing the wind farms, the maximum capacity of power generation needs to be pre-decided, as it impacts the logistics and capital cost.

The wind farm site selection requires analysis of many factors. They are described as follows:

- *Wind speed* is considered to be a critical parameter as it is affecting the wind power generation. The monthly and yearly average wind speed and variation mainly depends on location. For example, Sinden [I-6], based on data obtained from 66 onshore sites in the United Kingdom, concluded that the monthly average wind speed is inversely proportional to monthly average temperature. However, Hassanm and Hill [I-7] found that no such correlation exists at Dhahran, as temperature variation in Dhahran is small



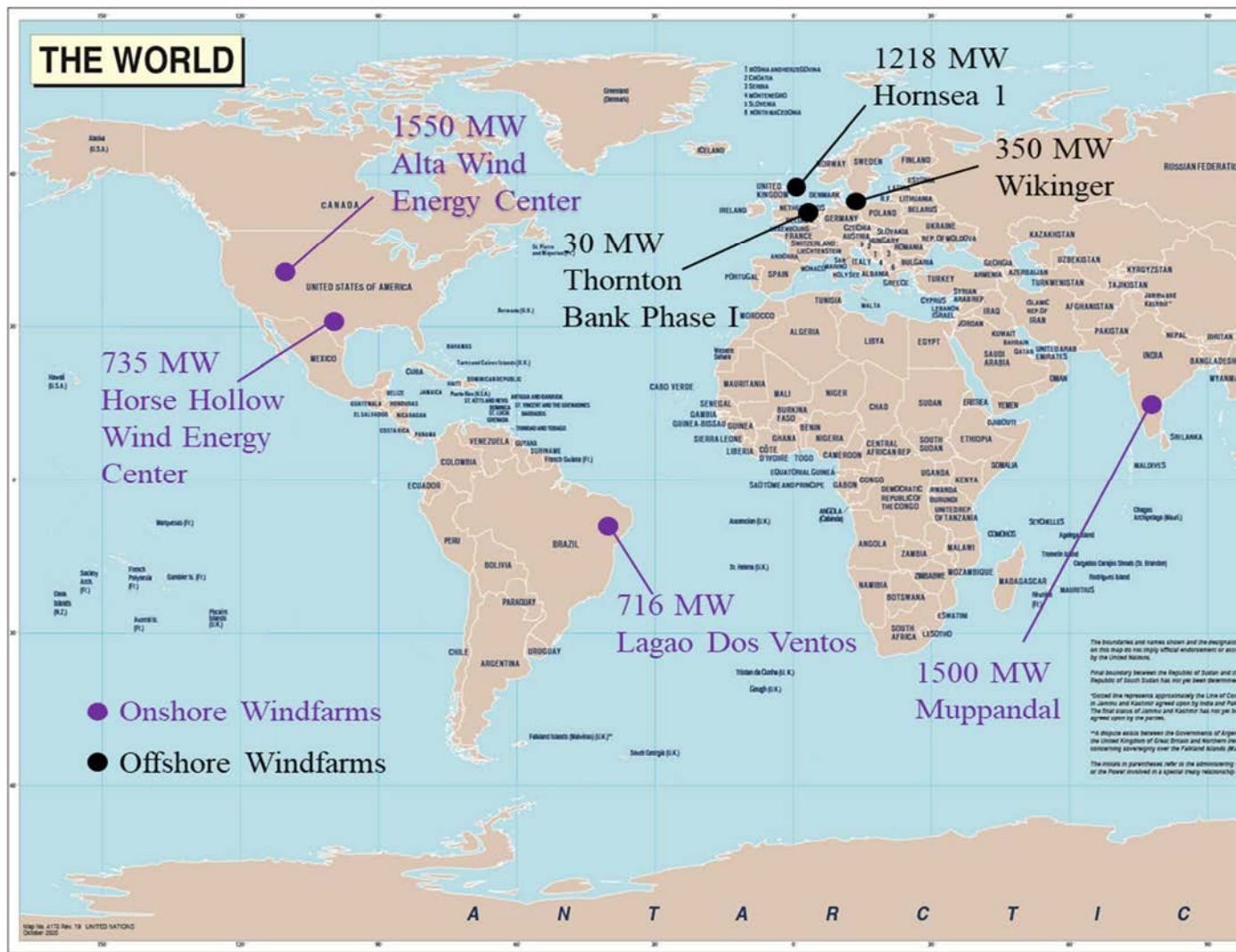


FIG. I-1. Onshore and offshore windfarms across the world<sup>1</sup>.

<sup>1</sup>UN map

over the year. Thus, the wind speed is a random variable, which is predicted using statistical methods such as Weibull distribution function [I-8].

- Apart from the wind speed, wind gust (sudden increase in wind speed in a very short time), needs to be considered while selecting the location. It is highly desirable to predict the wind gust at specific location for safe operation of the wind farm. Several methods are developed to predict the wind gusts [I-9, I-10].
- *Wind direction*: it is necessary to have data on statistical variation of wind direction for effective operation of the wind farm. Usually, a wind rose diagram is used for the analysis and prediction of the wind direction during the days, months, seasons, or years. Figure I-2 shows an example of a wind rose diagram. It represents the frequency of the wind direction in sixteen directions throughout the year [I-11].

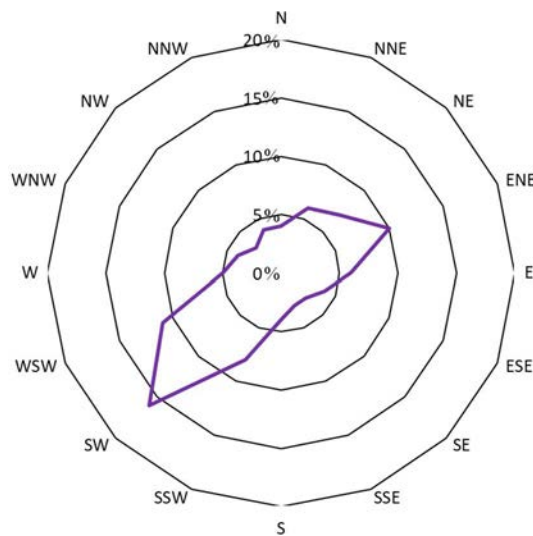


FIG. I-2: Example of a wind rose diagram.

- Noise pollution, wildlife, proximity of a windfarm to cities and airports, radar interferences, land cost, transport facilities, distance to electrical grid and social acceptance.
- A typical wind turbine is designed to follow general power curve as shown in Fig. I-3 at specified location [I-12]. It shows the variation of fractional output power with incoming wind speed. The cut-in speed is the minimum speed at which the wind turbine starts to rotate, whereas the cut-off speed is the maximum speed at which the wind turbine can operate. Due to structural limitations, the wind turbine cannot be operated at wind speed beyond the cut-off speed.
- *Determination of the wind turbine height to generate the required power capacity in a limited land area*: the wind speed and hence the power generation from the wind is greatly affected by the height of the turbine hub above the ground level. Doubled windspeed at turbine hub, increases the power generation by eight times. Because of strong dependence of windspeed with height above the ground level, the modern wind turbines have heights greater than 80 m, to extract maximum wind power with lower cost per unit power output. However, the maximum height of the wind turbine is limited

by material and structural constraints. The wind speed at different heights can be estimated with good accuracy using the Hallman power equation, which also considers the impact of surface roughness [I-11].

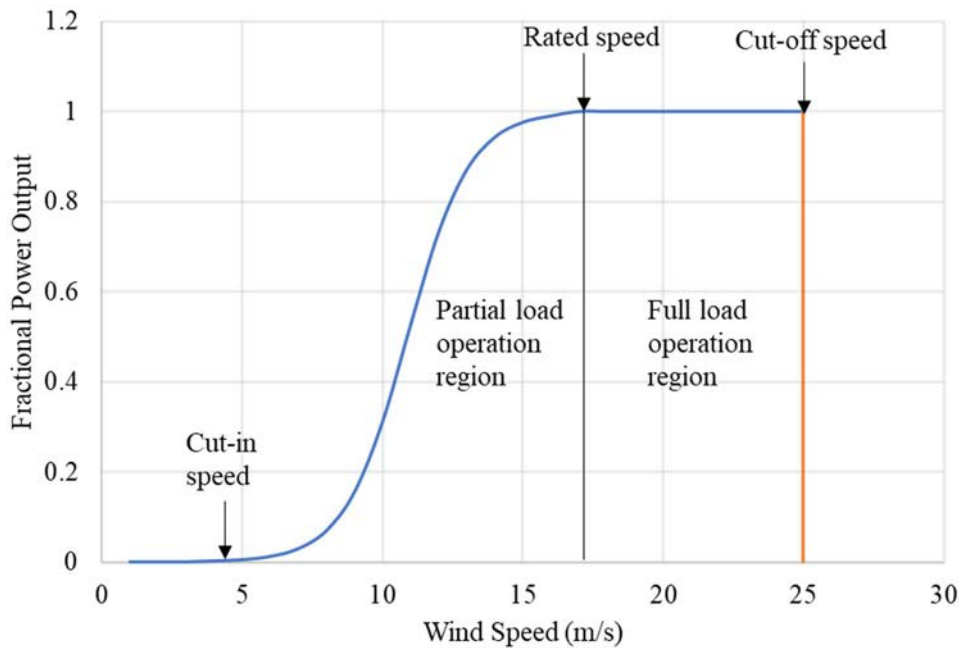


FIG. I-3: Generalized wind turbine power curve.

In designing the wind farms important aspect is the placement of wind turbines in the wind farm to generate the maximum possible energy. Figure I-4 shows a sketch of a hypothetical wind farm consisting of nine wind turbines placed in a square field. The field is divided into 36 equal cells and the wind turbines are placed in the cells in straight lines separated by a single cell. The wind direction is from north to south. The downstream wind from the first row of wind turbines acts as the upstream wind for row 3 wind turbines. Similarly, the downstream wind from row 3 wind turbines acts upstream wind for row 5 wind turbines. The power extracted from a wind turbine is maximum if the downstream wind speed is one third of the upstream wind speed [I-13]. If these turbines are to be placed exactly inline (one behind the other) without any gap in between, and operated for maximum power generation, then the upstream wind reaching the wind turbines in row 5 is 89 % slower than the wind speed upstream the wind turbines in row 1. Thus, greatly reducing the total power produced by the wind farm.

Figure I-5 shows another example of a hypothetical wind farm in which the wind turbines are staggered. Simply, by replacing the wind turbine in different location can enhance the efficiency as well as the power generation [I-14]. The only wind turbines in row 5 are inline with the wind turbines in row 1, and the separation between them is large, which greatly reduces the effect of upstream wind turbines. The interaction between the wakes produced by upstream turbines influences the overall efficiency of the wind farm, which results in very low power output as compared to the estimated power output [I-3]. Another limiting factor is land area, which needs to be utilized in best possible way to extract the maximum power. Several studies provide suggested optimum wind turbine locations [I-15 to I-17].

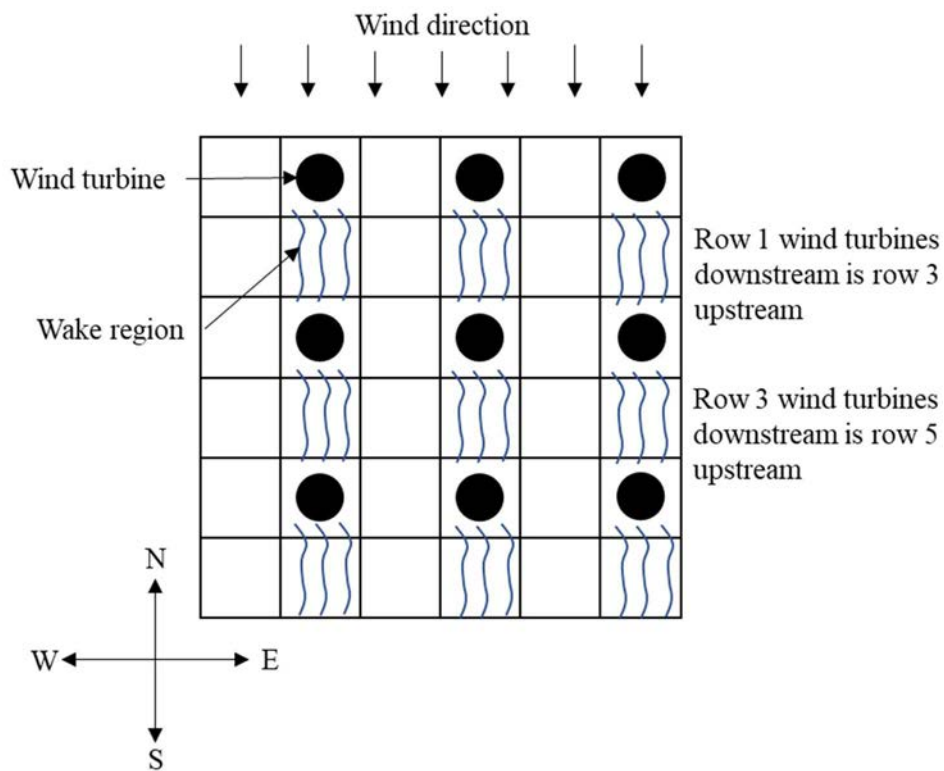


FIG. I-4. Layout of an inline wind farm.

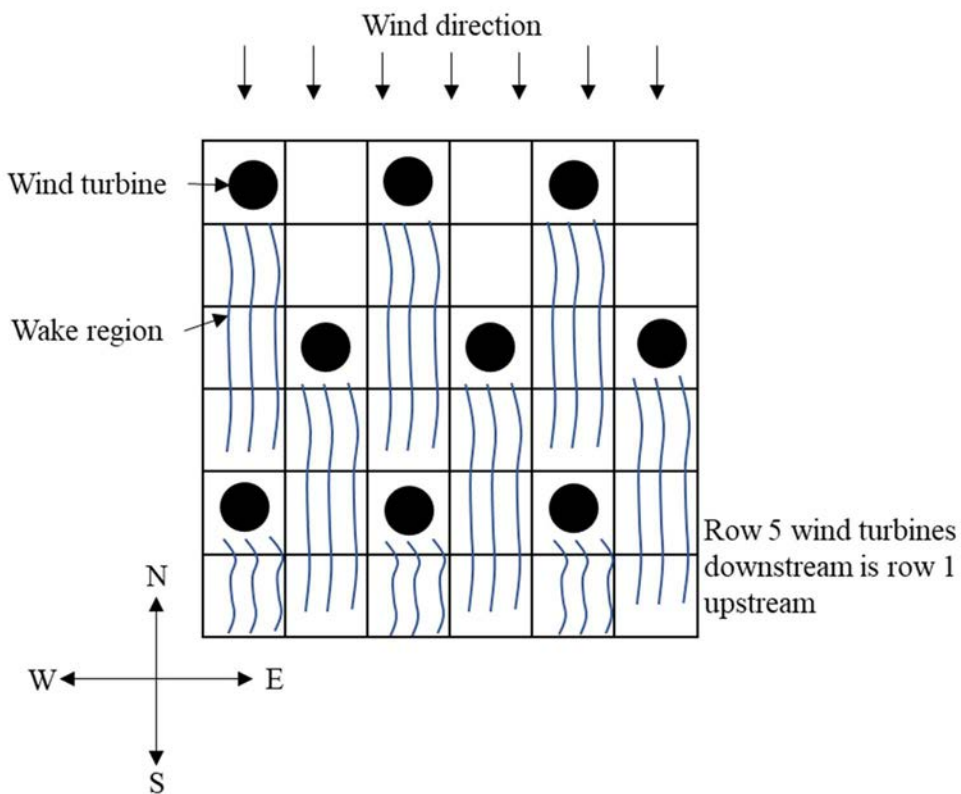


FIG. I-5. Layout of staggered wind farm.

### I-3. WIND FARM OPERATION

Figure I-6 shows a general layout of the wind turbine and its sub-components after the commissioning of the wind farm. The wind moves across the blades and rotate them; the blades are connected to the hub and low speed shaft. Both, the blades and the low speed shaft have same rotational speed (7 rpm–12 rpm). The rotational speed is increased using the gearbox between the high speed shaft and the low speed shaft. The high speed shaft rotates at about 1,500 rpm and is connected to the generator which converts mechanical energy into electrical energy. The produced electrical power is fed to the transformer which increases the voltage (22 kV–66 kV). The substation further increases the voltage (132 kV) and transfers the electricity to the distribution network, which then transports it to the end users [I-1]. All these components in the wind turbine need continuous monitoring and maintenance, especially the gearbox and the bearings of the generator.

The safe operation of all wind turbines in the wind farm needs to be ensured using the periodic inspections of all mechanical and electrical components and the analysis of potential risks associated with wind farms such as fire hazard, machine damage, bird strike, etc.

The wind turbines are usually operated and controlled automatically. The data of the wind speed, wind direction, rotational speed, electrical power, temperature, blade pitch, and other operational parameters is continuously stored and monitored using the system control and data acquisition software. It improves the efficiency of operation and provides the information about malfunctions. The bearings and the gear box are equipped with condition monitoring system to foresee the damage of the main drive train [I-1], and the bearings are lubricated periodically during the operational period of the wind farm.

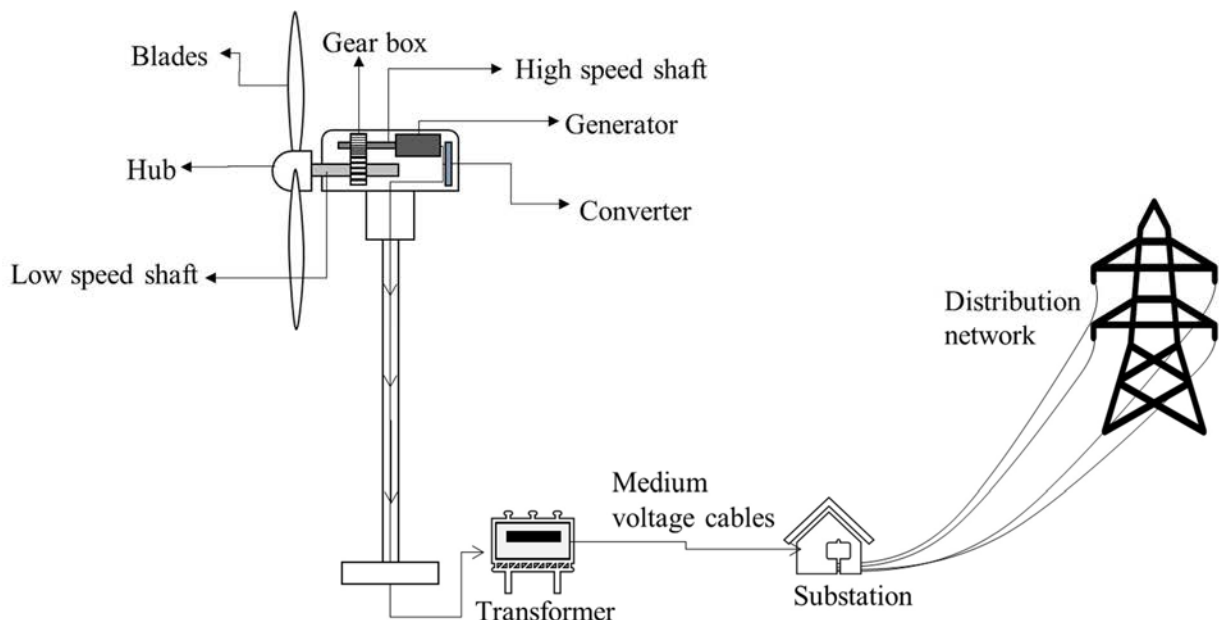


FIG. I-6. Schematic of wind turbine and wind farm components.

## REFERENCES TO ANNEX I

- [I-1] GASH, R., TWELE, J. (eds.), *Wind Power Plants: Fundamentals, Design, Construction and Operation*, Springer Science and Business Media, New York (2011).
- [I-2] THÖNNIBEN, F., et al., A numerical analysis to evaluate Betz's Law for vertical axis wind turbines, *Journal of Physics Conference Series* 2 **753** (2016) 022056.
- [I-3] HACES-FERNANDEZ, F., CRUZ-MENDOZA, M., LI, H., Onshore wind farm development: technologies and layouts, *Energies*, 7 **15** (2022) 2381.
- [I-4] INTERNATIONAL ENERGY AGENCY, *Wind Electricity*, IEA, Paris (2022).
- [I-5] DIAZ, H., SOARES, C. G., Review of the current status, technology and future trends of offshore wind farms, *Ocean Engineering* **209** (2020) 107381.
- [I-6] SINDEN, G., Characteristics of the UK wind resource: long-term patterns and relationship to electricity demand, *Energy Policy* 1 **35** (2007) 112, 127.
- [I-7] AL-HASSAN, A. Y., HILL, D. R., *Islamic Technology: An Illustrated History*, Cambridge University, UK (1986).
- [I-8] WEIBULL, W., A statistical distribution function of wide applicability, *ASME Journal of Applied Mechanics* 3 **18** (1951) 239, 297.
- [I-9] BRASSEUR, O., Development and application of a physical approach to estimating wind gusts, *Monthly Weather Review*, 1 **129** (200), pp. 5–25, 2001
- [I-10] MITSUTA, Y., TSUKAMOTO, O., Studies on spatial structure of wind gust, *Journal of Applied Meteorology* 11 **28** (1989) 1155, 1160.
- [I-11] TONG, W., *Fundamentals of Wind Energy*, WIT, UK (2010).
- [I-12] HALL, J. F., MECKLENBORG, C. A., CHEN, D., PRATAP, S. B., Wind energy conversion with a variable-ratio gearbox: design and analysis, *Renewable Energy* 3 **36** (2011) 1075, 1080.
- [I-13] RAGHEB, M., RAGHEB, A. M., Wind turbines theory-the betz equation and optimal rotor tip speed ratio, *Fundamental and Advanced Topics in Wind Power* 1 **1** (2011) 19, 38.
- [I-14] REDDY, S. R., Wind farm layout optimization (WindFLO): An advanced framework for fast wind farm analysis and optimization, *Applied Energy* **269** (2020) 115090.
- [I-15] CHEN, K., et al., Joint optimization of wind farm layout considering optimal control, *Renewable Energy* **182** (2022) 787, 796.
- [I-16] CAO, L., et al., Wind farm layout optimization to minimize the wake induced turbulence effect on wind turbines, *Applied Energy* **323** (2022) 119599.
- [I-17] TANG, X. Y., et al., Optimization of wind farm layout with optimum coordination of turbine cooperations, *Computers & Industrial Engineering* **164** (2022) 107880.



## ANNEX II

### HYDROGEN PRODUCTION

Hydrogen is known as technically feasible energy vector that can be used in several applications ranging from small scale power supply, zero emission fuel, energy storage devices to large scale chemical energy exports. Most of hydrogen available on earth is in form of compounds in combination with carbon as organic compounds or with oxygen as water. The industries rely heavily on fossil fuels (hydrocarbons) for the extraction of hydrogen (about 96% of the world's production), emitting CO<sub>2</sub> to the atmosphere [II-1]. However, new CO<sub>2</sub> free hydrogen production processes are needed to meet the energy market demands and to achieve zero greenhouse gases emission goal [II-2].

#### II-1. HYDROGEN PRODUCTION METHODS

Table II-1 summarizes several methods that are used in industries for hydrogen production and the required temperatures.

TABLE II-1. HYDROGEN PRODUCTION METHODS [II-2]

Hydrogen Production Method	Temperature Required (°C)
<b>Steam reforming:</b> Catalytic decomposition of light hydrocarbons with superheated steam	500–850
<b>CO<sub>2</sub> reforming:</b> Also known as dry reforming, is the catalytic decomposition of light hydrocarbons using CO <sub>2</sub>	800–1,000
<b>Partial oxidation:</b> Chemical reaction between carbonaceous feedstock and sub-stoichiometric pure oxygen	900–1,450
<b>Steam-coal gasification:</b> Two-step process that involves pyrolysis reaction and the water-gas reaction	400–600
<b>Steam-biomass gasification:</b> Two-step process that involves biomass thermal decomposition followed by hydrocarbon gas and carbon reactions with CO, CO <sub>2</sub> , H <sub>2</sub> and H <sub>2</sub> O	600–900
<b>Low temperature electrolysis:</b> Dissociation of water into H <sub>2</sub> and O <sub>2</sub> in presence of liquid or solid electrolyte by applying electrical current	< 150
<b>High temperature electrolysis:</b> Variant of low temperature electrolysis with less electrical and high thermal input	800–1,000

#### II-2. NUCLEAR HYDROGEN PRODUCTION

Dominant method for hydrogen production in industries is steam reforming, which can be a starting point for coupling the steam reforming process with high temperature gas cooled reactor for fossil free hydrogen production [II-2]. It can result in 40% savings of natural gas feedstock if the primary heat is taken from nuclear reactor [II-3]. However, the safety requirements for using the nuclear steam reforming are much more stringent than for the fossil



fuel based systems. Several experimental studies were performed simulating nuclear conditions to study the feasibility of hydrogen production with high temperature gas cooled reactor. A specially designed steam reformer is used to transfer heat from the primary coolant to the feed gas for hydrogen production, which prevents the primary coolant permeation to the hydrogen production facility [II-2].

The steam reformer can be coupled with high temperature gas reactor through the intermediate heat exchanger as shown in Fig. II-2. This approach has been used in Japan's HTTR project which shows the world's first potential nuclear steam reformer system using high temperature engineering test reactor coupled with hydrogen production facility through the intermediate heat exchanger and steam reformer. The separation between the nuclear power plant and hydrogen production facility avoids possible contamination and reduces the tritium penetration [II-2].

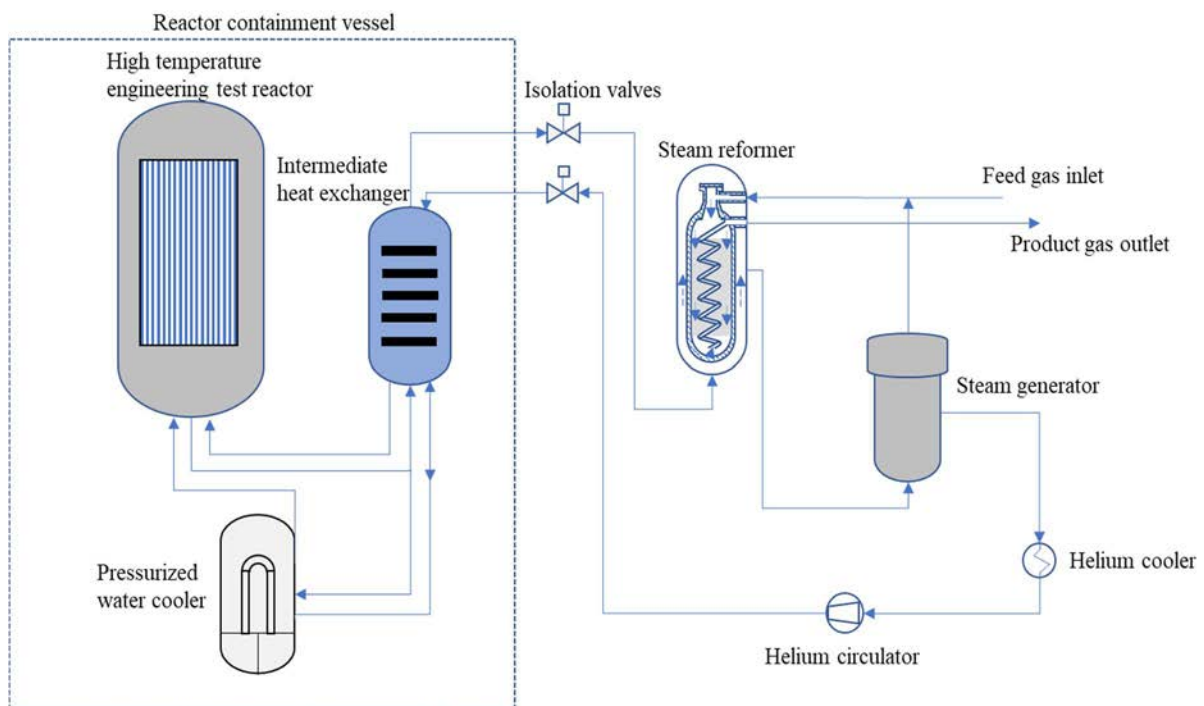


FIG. II-2. Schematic of nuclear steam reforming system.

Another technologically common method for hydrogen production is low temperature electrolysis. Several industrial plants are producing the hydrogen across the world using this method (e.g., De Nora, Lurgi and Proton HOGEN) [II-2]. The technology for low temperature electrolysis is well developed and can be used with evolutionary water-cooled reactors by utilizing the electricity for producing hydrogen. Since the process can be decoupled from the nuclear power plant, it allows decentralized hydrogen production and can serve as a transition towards green energy production. Apart from this, several countries have also started the experimental activities on use of high temperature electrolysis, which is focused on development, optimization and coupling of different electrolysis cells with nuclear heat source [II-2]. The other methods for nuclear hydrogen production that are currently under research are listed below:

- Nuclear steam gasification;
- Biomass thermochemical conversion using high temperature gas cooled reactor;
- Thermochemical cycle.

#### REFERENCES TO ANNEX II

- [II-1] SCHOLZ, W.H., Verfahren zur großtechnischen Erzeugung von Wasserstoff und ihre Umweltproblematik, Linde Berichte aus Technik und Wissenschaft **67** (1992) 13–21.
- [II-2] INTERNATIONAL ATOMIC ENERGY AGENCY, Hydrogen Production Using Nuclear Energy, NP-T-4.2, IAEA, Vienna (2013).
- [II-3] SPATH, P.L., MANN, M.K., Life Cycle Assessment of Hydrogen Production via Natural Gas Steam Reforming, Report NREL/TP-570-27637, National Renewable Energy Laboratory, Golden, CO, United States (2001).



## **CONTRIBUTORS TO DRAFTING AND REVIEW**

Ahmad, A.	Pakistan Institute of Engineering and Applied Sciences
Ali, B.	Pakistan Institute of Engineering and Applied Sciences
Jevremovic, T.	International Atomic Energy Agency
Rasheed, K.	Pakistan Institute of Engineering and Applied Sciences
Rehman, H ur.	International Atomic Energy Agency
Riaz, W.	International Atomic Energy Agency
Sungur, N.	International Atomic Energy Agency





## ORDERING LOCALLY

IAEA priced publications may be purchased from the sources listed below or from major local booksellers.

Orders for unpriced publications should be made directly to the IAEA. The contact details are given at the end of this list.

### NORTH AMERICA

***Bernan / Rowman & Littlefield***

15250 NBN Way, Blue Ridge Summit, PA 17214, USA

Telephone: +1 800 462 6420 • Fax: +1 800 338 4550

Email: [orders@rowman.com](mailto:orders@rowman.com) • Web site: [www.rowman.com/bernan](http://www.rowman.com/bernan)

### REST OF WORLD

Please contact your preferred local supplier, or our lead distributor:

***Eurospan Group***

Gray's Inn House  
127 Clerkenwell Road  
London EC1R 5DB  
United Kingdom

***Trade orders and enquiries:***

Telephone: +44 (0)176 760 4972 • Fax: +44 (0)176 760 1640

Email: [eurospan@turpin-distribution.com](mailto:eurospan@turpin-distribution.com)

***Individual orders:***

[www.eurospanbookstore.com/iaea](http://www.eurospanbookstore.com/iaea)

***For further information:***

Telephone: +44 (0)207 240 0856 • Fax: +44 (0)207 379 0609

Email: [info@eurospangroup.com](mailto:info@eurospangroup.com) • Web site: [www.eurospangroup.com](http://www.eurospangroup.com)

### Orders for both priced and unpriced publications may be addressed directly to:

Marketing and Sales Unit

International Atomic Energy Agency

Vienna International Centre, PO Box 100, 1400 Vienna, Austria

Telephone: +43 1 2600 22529 or 22530 • Fax: +43 1 26007 22529

Email: [sales.publications@iaea.org](mailto:sales.publications@iaea.org) • Web site: [www.iaea.org/publications](http://www.iaea.org/publications)











INTERNATIONAL ATOMIC ENERGY AGENCY  
VIENNA